

Reproduction of charmed mesons at 2.76 and 5.02 TeV

Huanjing Gong^{1,*}

¹Department of Physics, Sichuan University, Chengdu 610064, China

(Dated: June 19, 2023)

I. BACKGROUND

Previously, we reproduce charmed meson ($J/\psi, D^0, D_s$) successfully in the Au Au collision at 200 GeV in the Recombination Model framework, seen in Figs.1, 2, 3. Thus, they are anticipated to be reproduced in the Pb Pb collision at 2.76 TeV and 5.02 TeV.

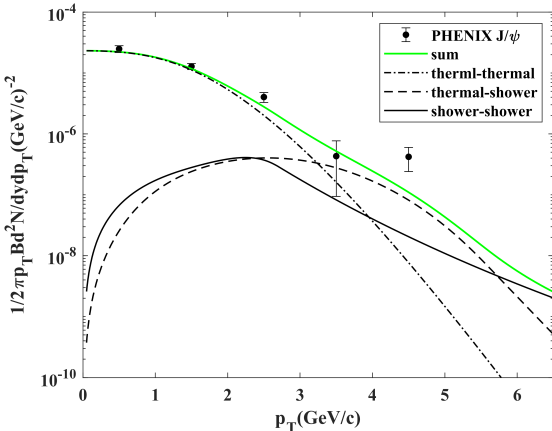


FIG. 1: Transverse momentum spectra of J/ψ at 200 GeV.

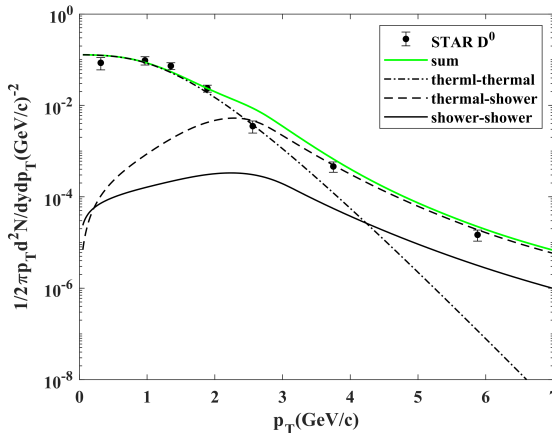


FIG. 2: Transverse momentum spectra of D^0 at 200 GeV.

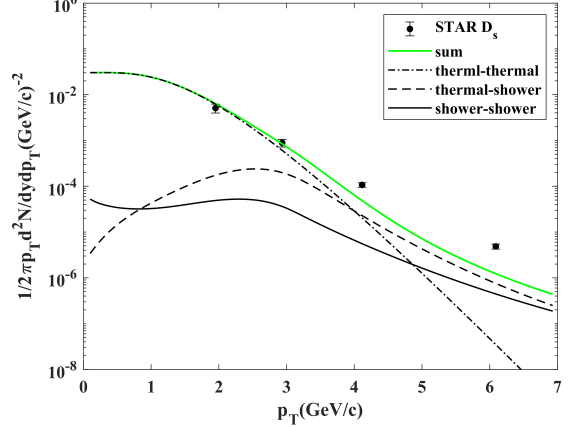


FIG. 3: Transverse momentum spectra of D_s at 200 GeV.

II. URGENT QUESTIONS

Data for $J/\psi, D^0, D_s$ at $\sqrt{s_{NN}}=2.76/5.02$ TeV are found in the form of dN/dp_T [4–9], which need to be multiplied by $1/2\pi p_T$. Change of energy only leads to the various coefficients in $f_i(k)$, which has impact on TT and TS terms. Moreover, some parameters, e.g. $\gamma, v_T, \beta L, ect$, may need to be reoptimized.

As for $f_i(k)$, parameters for the initial hard parton distribution at $\sqrt{s_{NN}}=200$ GeV (RHIC) and 5.5 TeV (LHC) are available in [1, 2], which are not certainly reliable at $\sqrt{s_{NN}}=2.76/5.02$ TeV.

$$f_i(p_T) = \frac{dN^{jet}}{d^2p_T dy} = K \frac{C}{(1 + p_T/B)^\beta} \quad (1)$$

For $u, \bar{u}, d, \bar{d}, g, s, \bar{s}$ quark, we can obtain parameters at 2.76 and 5.02 TeV by logarithmic interpolations between 200 GeV and 5.5 TeV for $\ln A, B, \beta$ [3], whereas parameters for c/\bar{c} are still not known. Following the notion in [3], we get the parameters in Eq.1 at 2.76 and 5.02 TeV.

The initial p_T spectra of charm quarks at midrapidity at 200 GeV is taken to be

$$f_c(p_T) = \frac{dN_c}{d^2p_T} = \frac{19.2 [1 + (p_T/6)^2]}{(1 + p_T/3.7)^{12} [1 + \exp(0.9 - 2p_T)]} \quad (2)$$

which is obtained by multiplying the heavy quark p_T spectra from p+p collisions at same energy by the number of binary collisions (~ 960) in Au+Au collisions [2].

For LHC energies (5.5 TeV) we take the initial p_T spectra of charm quark at midrapidity from the perturbative

*Electronic address: gonghuanjing@qq.com

calculation multiplied by the number of binary collisions (~ 1700) [10].

$$\begin{aligned} f_c(p_T) &= \frac{dN_c}{d^2 p_T} \\ &= 2497(1 + \frac{p_T}{1.95})^{-5.5} \left(p_T \left[1 + \left(\frac{4}{0.1 + p_T} \right)^2 \right] \right)^{-1} \end{aligned}$$

Thus, we now just use the formula at 5.5 TeV for 2.76/5.02 TeV, as it is rough to generalize them to 2.76/5.02 TeV.

Besides, while it is negligible at $\sqrt{s_{NN}}=200$ GeV, the new component of the two-jet contribution $SS(2)$ should be taken into account at $\sqrt{s_{NN}}=2.76/5.02$ TeV, which is given by [11]

$$\begin{aligned} \frac{dN^{SS(2)}}{dp dp} &= \frac{1}{p^0 p} \sum_{i,i'} \int \frac{dq}{q} \frac{dq'}{q'} F_i(q) F_{i'}(q') \Gamma(q, q') \quad (4) \\ &\times \int \frac{dp_1}{p_1} \frac{dp_2}{p_2} F_{ii'}(q, q'; p_1, p_2) R_M(p_1, p_2, p). \end{aligned}$$

More details are shown in the next section. Then, the first results are shown in Figs. 4, 5, 6.

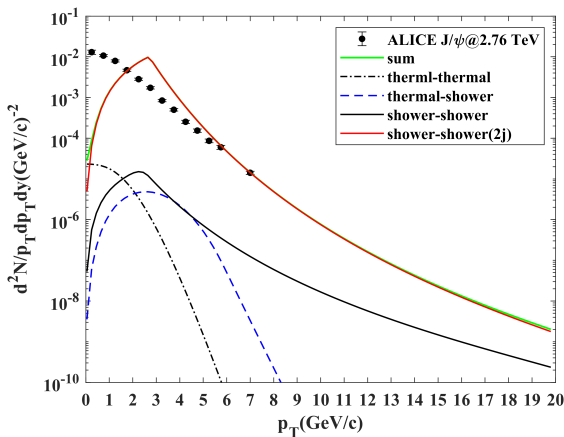


FIG. 4: Transverse momentum spectra of J/ψ at 2.76 TeV with $\Gamma = 10^{-3}$.

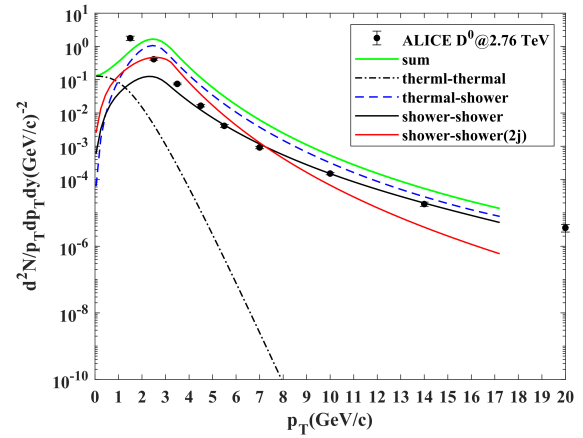


FIG. 5: Transverse momentum spectra of D^0 at 2.76 TeV with $\Gamma = 10^{-3}$.

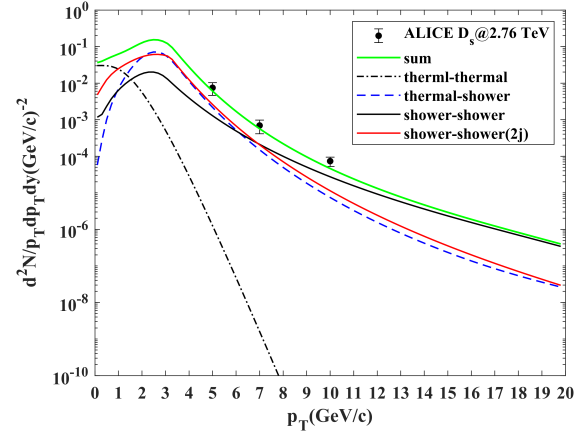


FIG. 6: Transverse momentum spectra of D_s at 2.76 TeV with $\Gamma = 10^{-3}$.

III. FIT AND OPTIMIZATION

Since last meeting, two ideas are put forward. First, the contribution TT should be optimized by fitting η_T . Second, $f_i(k)$ in Pb+Pb at 2.76 and 5.02 TeV should be given, which cannot be replaced by that at 5.5 TeV.

As a result, we find that the change of v_T can effect only one order of magnitude of TT . But the running mass of charm does matter in T composition. The change m_c from 1.5 to 1.2 can fit the data at least in TT , although $v_T = 0.1c$ and $\gamma_c = 1.1$ can also fit the data. Consequently, we fix $\gamma_c = 0.26$, $v_T = 0.25c$, temperature $T = 0.185$ GeV and $m_c = 1.28$, fitted by thermal parton distribution at low p_T .

Here, we give the four contributions again as follows. And notice that the results of TS , $SS(1j)$, $SS(2j)$ terms are multiplied by a factor of $1 - e^{-p/2}$ to suppress the low p contribution.

A. TT term

$$\frac{dN_M^{TT}}{d^2p} = C_M M_T \frac{\tau A_T}{(2\pi)^3} 2\gamma_a \gamma_b I_0 \left[\frac{psinh\eta_T}{T} \right] \times \int_0^1 dx |\phi_M(x)|^2 k_M(x, p), \quad (5)$$

where

$$k_M(x, p) = K_1 \left[\frac{cosh\eta_T}{T} (\sqrt{m_a^2 + p_1^2} + \sqrt{m_b^2 + p_2^2}) \right] \quad (6)$$

$$|\phi_M(x)|^2 = \frac{1}{B(a, b)} x^{a-1} (1-x)^{b-1} \quad (7)$$

and $p_1 = xp$, $p_2 = (1-x)p$, $A_T = \rho_0^2 \pi$ with the radius $\rho_0 = 9$ fm, the meson degeneracy factor $C_M = (2 \times 3)^2$. It was assumed that hadronization occurs at $\tau = 5$ fm with temperature $T = 0.175$ GeV in the parton phase. I_0 and K_1 are the modified Bessel functions. Moreover, the fugacities of light quarks are $\gamma_u = \gamma_d = 1$ and for the strange quarks $\gamma_s = 0.8$. The free parameters are fugacity $\gamma_c = 0.26$ (fixed) and transverse flow rapidity η_T defined by a flow velocity with $v_T = tanh\eta_T$. Fitted by experimental data in Au+Au collision at RHIC energy, we have obtained $v_T = 0.3c(J/\psi)$ and $v_T = 0.42c(D^0)$.

B. TS term

$$\frac{dN_M^{TS}}{d^2p} = C_M \int_0^1 dx |\phi_M(x)|^2 \times \left[\frac{T_a(p_1)S_b(p_2)}{g\gamma_a x} + \frac{S_a(p_1)T_b(p_2)}{g\gamma_b(1-x)} \right] \quad (8)$$

with $g = 6$ coming from the color and spin degeneracy of a quark. And the thermal parton spectrum

$$T_a(p) = \frac{2g\gamma_a m_T}{(2\pi)^3} I_0 \left[\frac{psinh\eta_T}{T} \right] K_1 \left[\frac{m_T cosh\eta_T}{T} \right]. \quad (9)$$

Then, the the distribution of shower parton j

$$S_j(p) = \sum_i \int \frac{dq}{q} F_i(q) S_i^j(p/q), \quad (10)$$

where

$$F_i(q) = \frac{1}{\beta L} \int_q^{qe^{\beta L}} \frac{dk}{k} f'_i(k), \quad (11)$$

with $f'_i(k) = f_i(k)(2\pi)^3/E$.

C. $SS(1j)$ term

$$\frac{dN_M^{SS(1)}}{pdः} = \frac{1}{p^0 p} \sum_i \int \frac{dq}{q} F'_i(q) \frac{p}{q} D_i^M(\frac{p}{q}), \quad (12)$$

where

$$F'_i(q) = \frac{1}{\beta L} \int_q^{qe^{\beta L}} dk k f_i(k), \quad (13)$$

and D_i^M is the FF of quark i splitting into meson M.

$$xD_i^H(x) = \int_0^x \frac{dx_1}{x_1} \int_0^x \frac{dx_2}{x_2} \{S_i^q(x_1), S_i^{\bar{q}'}(x_2)\} R(x_1, x_2, x) \quad (14)$$

D. $SS(2j)$ term

Besides, while it is negligible at $\sqrt{s_{NN}}=200$ GeV, the new component of the two-jet contribution $SS(2)$ should be taken into account at $\sqrt{s_{NN}}=2.76/5.02$ TeV, which is given by [11]

$$\begin{aligned} \frac{dN^{SS(2)}}{pdः} &= \frac{1}{p^0 p} \sum_{i,i'} \int \frac{dq}{q} \frac{dq'}{q'} F'_i(q) F'_{i'}(q') \Gamma(q, q') \\ &\times \int \frac{dp_1}{p_1} \frac{dp_2}{p_2} F_{ii'}(q, q'; p_1, p_2) R_M(p_1, p_2, p). \end{aligned} \quad (15)$$

In the above expression, $F_{ii'}$ is the distribution of shower partons related to the two jets and for a meson it is written as

$$F_{ii'}(q, q'; p_1, p_2) = S_i^j(\frac{p_1}{q}) S_{i'}^{j'}(\frac{p_2}{q'}), \quad (16)$$

and since we have not sufficient information of such dependencies for collisions at LHC, the overlap function is approximated by an average quantity Γ which varies over a wide range $\Gamma = 10^{-n}$ with $n = 1, 2, 3$ and 4.

Specifically, we simply the formulae of 3 mesons respectively for numerical computing as follows:

$$\begin{aligned} \frac{dN_{J/\psi}^{SS(2)}}{pdः} &= \frac{10^{-n}}{p^0 p} \sum_{\substack{i=g,c \\ i'=g,c}} \int \frac{dq}{q} \frac{dq'}{q'} F'_i(q) F'_{i'}(q') \\ &\times S_i^{\bar{c}}(\frac{p}{2q}) S_{i'}^c(\frac{p}{2q'}), \end{aligned} \quad (17)$$

$$\begin{aligned} \frac{dN_{D^0}^{SS(2)}}{pdः} &= \frac{5 * 10^{-n}}{p^0 p^6} \sum_{\substack{i=q,\bar{q},g \\ i'=g,c}} \int \frac{dq}{q} \frac{dq'}{q'} F'_i(q) F'_{i'}(q') \\ &\times \int_0^q dp_2 S_i^{\bar{u}}(\frac{p-p_2}{q}) S_{i'}^c(\frac{p_2}{q'}) p_2^4, \end{aligned} \quad (18)$$

$$\frac{dN_{D_s}^{SS(2)}}{dpdp} = \frac{660 * 10^{-n}}{p^0 p^{13}} \sum_{\substack{i=q,\bar{q},g,s,\bar{s} \\ i'=g,c}} \int \frac{dq}{q} \frac{dq'}{q'} F'_i(q) F'_{i'}(q') \times \int_0^q dp_2 S_i^{\bar{s}} \left(\frac{p-p_2}{q}\right) S_{i'}^c \left(\frac{p_2}{q'}\right) p_2^9 (p-p_2)^2 \quad (19)$$

To testify the accuracy of calculations, we reproduce the results (transverse momentum spectra for J/ψ at 5.5 TeV) in Ref.[11], shown in Fig.7, which has a good agreement with the reference.

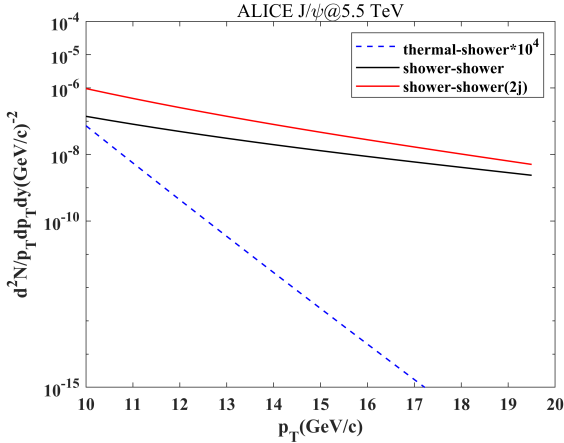


FIG. 7: The comparison of three terms for J/ψ at 5.5 TeV with $\Gamma = 10^{-2}$.

IV. SOLUTION OF HARD PARTON DISTRIBUTIONS FOR CHARM

After search and contacting some professors, it seems no one had studied parameterized initial charm quark distribution. Thus, we attempt to figure out interpolated functions at 2.76/5.5 TeV between 200 GeV and 5.5 TeV to solve it.

Because of known formula of u quark, we compare the parameterized results at various energy, shown in Fig. 8. Obviously, $\ln(f_i(k))$ is not linear with $\sqrt{s_{NN}}$, otherwise the curve of 2.76 TeV should be almost at the position where two curves of 5.5 TeV and 0.2 TeV are bisected. For simplicity, it is assumed that $\ln(f_i^{\sqrt{s}}(k))$ is linear with $\ln(\sqrt{s_{NN}})$ (in TeV), i.e. $f_i^{\sqrt{s}}(k)$ increases linearly with $\sqrt{s_{NN}}$. Therefore, hard parton distribution at any energy can be expressed:

$$\frac{f_i^{\sqrt{s}} - f_i^{5.5}}{\sqrt{s} - 5.5} = \frac{f_i^{0.2} - f_i^{5.5}}{0.2 - 5.5} \quad (20)$$

Then, we give the deviation between our linear evaluation and parameterized values in Fig.9, from which it is reasonable to accept the linear assumption. So we generalize this simple relation to initial charm quark distribution and get the distributions at 2.76 and 5.02 TeV successfully by linear combination of distributions at 0.2 and

5.5 TeV, shown in Fig.10. We also give another results assuming $\ln(f_i(k))$ is linear with $\sqrt{s_{NN}}$ to trial, shown in Fig.11.

Subsequently, we test the two $f_i(k)$, which is linear or exponential with $\sqrt{s_{NN}}$ respectively, by calculating the momentum spectra for J/ψ at 2.76 TeV shown in Fig.12 and 13. Unfortunately, the former result, which should be logically compelling, is even worse than the latter, and both of all cannot fit the experiment data. But the latter conveys that the dominant components $SS(1j)$ and $SS(2j)$ in high transverse momentum determine the accuracy of fitting. And next step should be to determine further the shape of $f_i(k)$ for charm.

After that, from the high contribution of SS , it is reasonable to decrease $f_i(k)$ of charm. Therefore, we adjust the weight of $f_c(k)$ at 200 GeV from about 0.51, according to Eq.20, to 0.6 shown in Fig.14, improving the calculated p_T distribution for $J/\psi, D^0, D_s$ at 2.76 TeV shown in Figs.15, 16, 17. The parameters changed are list here:

$$J/\psi : v_T = 0.25c, T = 0.185 \text{ GeV}, \Gamma = 5 \times 10^{-3}, \quad (21)$$

$\beta L \rightarrow 0$ for charm, 2.39 for gluon

$$D^0 : v_T = 0.43c, T = 0.185 \text{ GeV}, \Gamma = 10^{-2}, \quad (22)$$

$\beta L = 5.8$ for all

$$D_s : v_T = 0.3c, T = 0.185 \text{ GeV}, \Gamma = 10^{-2}, \quad (23)$$

$\beta L = 5.0$ for all.

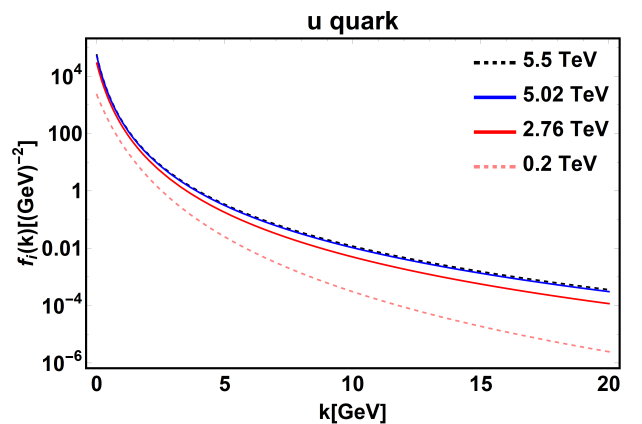


FIG. 8: Hard parton distribution of u quark at various energy.

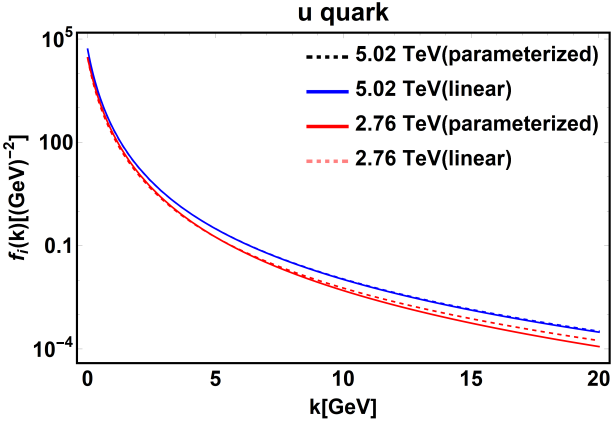


FIG. 9: Deviation between linear evaluation and parameterized values for u quark at 2.76 and 5.02 TeV.

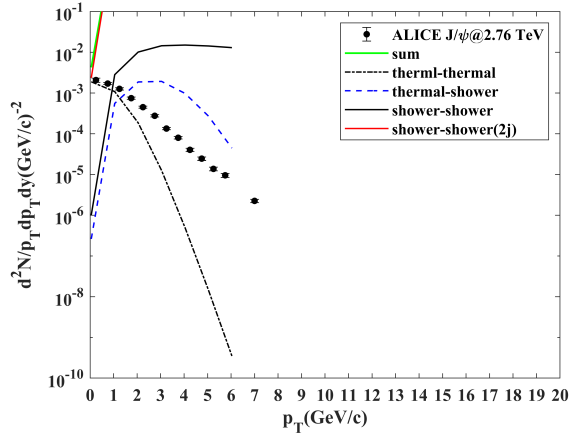


FIG. 12: J/ψ distribution at 2.76 TeV assuming $f_c(k)$ is linear with $\sqrt{s_{NN}}$.

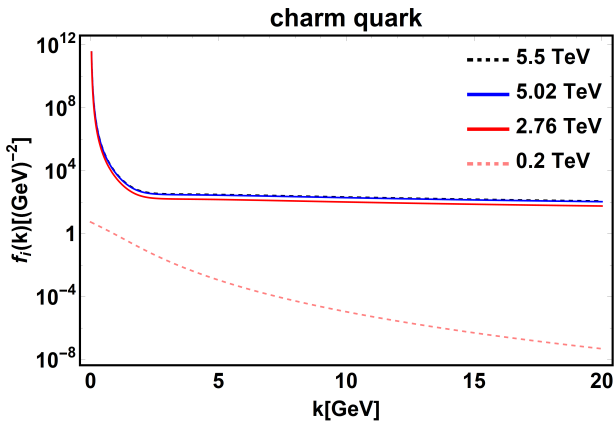


FIG. 10: Hard parton distribution of charm quark at various energy assuming $f_c(k)$ is linear with $\sqrt{s_{NN}}$.

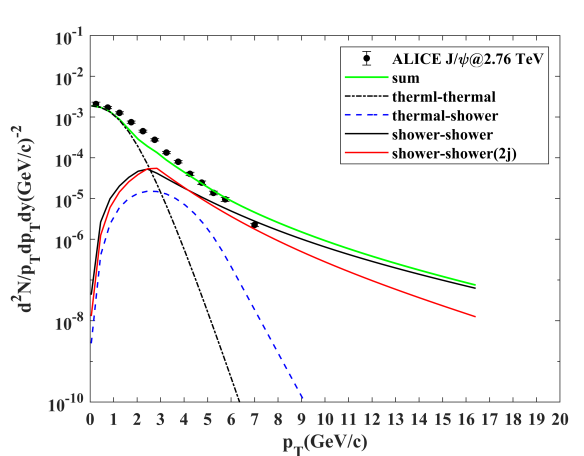


FIG. 13: J/ψ distribution at 2.76 TeV assuming $f_c(k)$ is exponential with $\sqrt{s_{NN}}$.

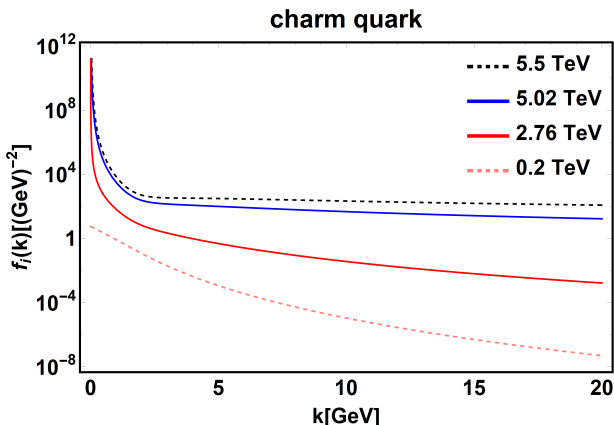


FIG. 11: Hard parton distribution of charm quark at various energy assuming $\ln(f_c(k))$ is linear with $\sqrt{s_{NN}}$.

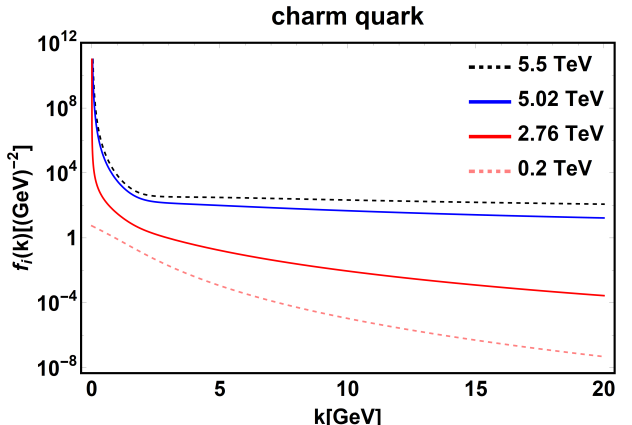


FIG. 14: Hard parton distribution of charm quark at various energy assuming $f_c(k) = 0.6f_c^{0.2}(k) + 0.4f_c^{5.5}(k)$.

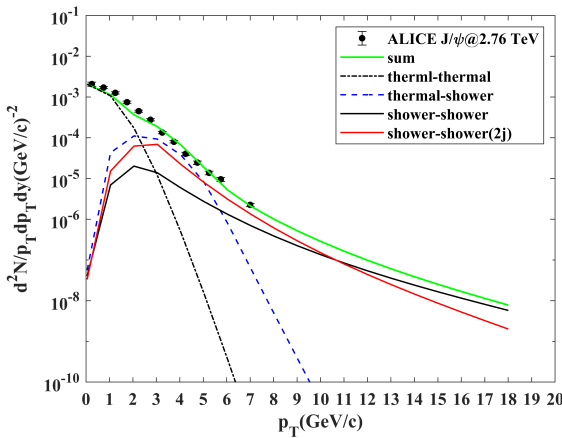


FIG. 15: J/ψ distribution at 2.76 TeV applying improved $f_c(k)$.

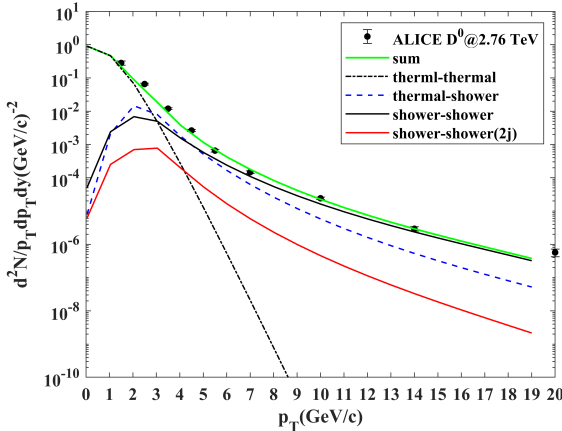


FIG. 16: D^0 distribution at 2.76 TeV applying improved $f_c(k)$.

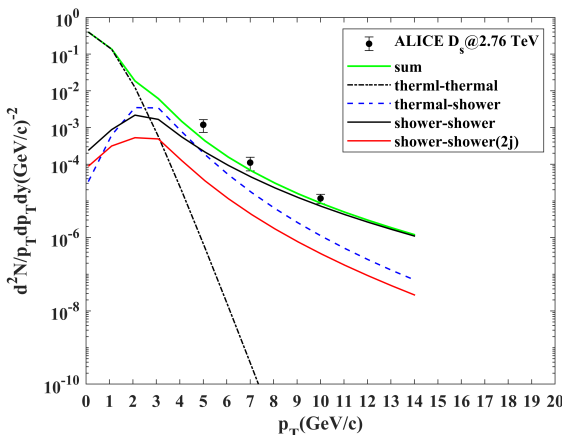


FIG. 17: D_s distribution at 2.76 TeV applying improved $f_c(k)$.

V. MEETING 2022.10.24

Last week, we improved the program by adopting $R_{J/\psi} = \frac{x_1 x_2}{x^2} \delta(\frac{x_1+x_2}{x} - 1)$ instead of $\frac{x_1 x_2}{x^2} \delta(\frac{x_1}{x} - \frac{1}{2}) \delta(\frac{x_2}{x} - \frac{1}{2})$ owing to interaction between c and \bar{c} quark. However, now we still adopt the latter form and $m_c = 1.5$ GeV to be consistent with Ref.[11]. Moreover, we should limit the p_T spectra in the range of 0 to 10 GeV to raise the program operating speed.

Besides, we fix the hard jet momentum limits q in shower parton distribution in the range of after checking *recomb_product_v15.f90*. Next we will improve the $SS(1)$ term and reproduce $J/\psi, D^0, D_s$ at 2.76 and 5.02 TeV, and figure out the issue of $SS(2)$ which shows a sharp decrease at point of changing integration low limit in Fig.18.

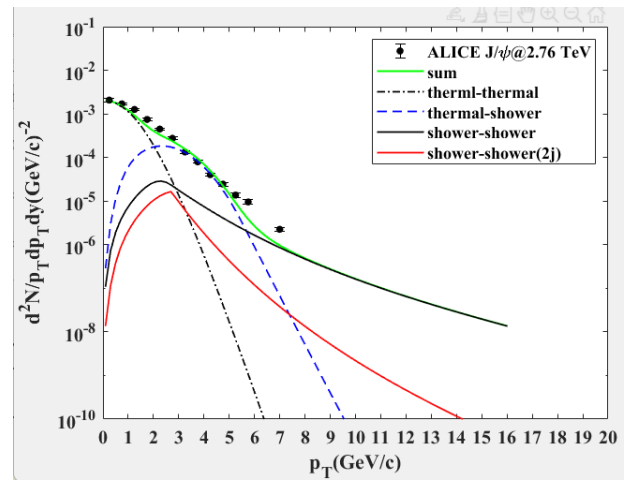


FIG. 18: J/ψ distribution at 2.76 TeV at 2022/10/24 meeting.

VI. MEETING 2022.10.31

Last week, we attempt to fit TT and TS terms by adopting $R_{J/\psi} = \frac{x_1 x_2}{x^2} \delta(\frac{x_1}{x} - \frac{1}{2}) \delta(\frac{x_2}{x} - \frac{1}{2})$ and $m_c = 1.5$ GeV. However, we find it hard to fit so we still use $m_c = 1.28$ GeV and change $R_{J/\psi}$ back only. Then, we improve the integrate limits in Eq.26 from 3 to 15 GeV and the critical point is changed to $p_T = 2q$.

Besides, trying to add cutoff in reference of [3] and [12], we find it analogous to add either $1 - e^{-p/2}$ or the cutoff. It is much lower if two factor are both added to suppress the low p_T contribution. Therefore, the cutoff are abandoned.

This week, J/ψ distribution is improved, shown in Fig.19, in which parameters at 2.76 TeV are listed here

in comparison with them at 200 GeV:

$$\begin{aligned} J/\psi \text{ at } 2.76 \text{ TeV} : v_T &= 0.25c, \gamma_c = 0.26, \\ T &= 0.185 \text{ GeV}, \Gamma = 10^{-2}, \end{aligned} \quad (24)$$

$\beta L \rightarrow 0$ for charm, 2.39 for gluon.

$$\begin{aligned} J/\psi \text{ at } 200 \text{ GeV} : v_T &= 0.3c, \gamma_c = 0.26, \\ T &= 0.175 \text{ GeV}, \\ \beta L &\rightarrow 0 \text{ for charm, 2.39 for gluon.} \end{aligned} \quad (25)$$

The results have a good agreement with ALICE data. And we will begin to focus on D^0, D_s at 2.76 TeV next. That will be easier.

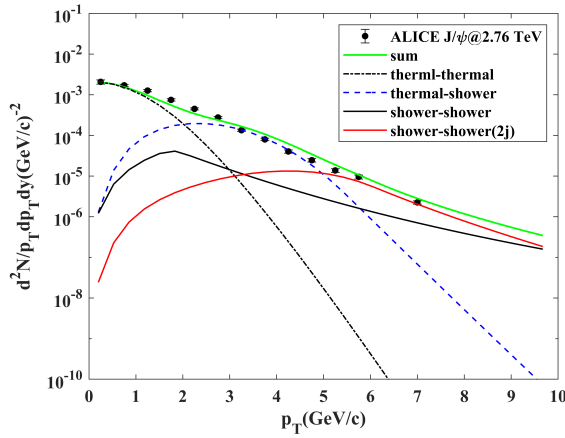


FIG. 19: J/ψ distribution at 2.76 TeV at 2022/10/31 meeting.

limit 2 will lead to $\frac{p}{q} > 1$.

$$\begin{aligned} \frac{dN_{J/\psi}^{SS(2)}}{pdः} &= \frac{10^{-n}}{p^0 p} \int_2^{30} \int_2^{30} \sum_{\substack{i=g,c \\ i'=g,c}} \frac{dq}{q} \frac{dq'}{q'} F_i'(q) F_{i'}'(q') \\ &\times S_i^c(\frac{p}{2q}) S_{i'}^c(\frac{p}{2q'}) \end{aligned} \quad (27)$$

$$\begin{aligned} \downarrow \\ \downarrow \text{when } p > 2 \\ \downarrow \\ \frac{dN_{J/\psi}^{SS(2)}}{pdः} &= \frac{10^{-n}}{p^0 p} \int_p^{30} \int_p^{30} \sum_{\substack{i=g,c \\ i'=g,c}} \frac{dq}{q} \frac{dq'}{q'} F_i'(q) F_{i'}'(q') \\ &\times S_i^c(\frac{p}{2q}) S_{i'}^c(\frac{p}{2q'}) \end{aligned} \quad (28)$$

The results are shown in Fig. 20.

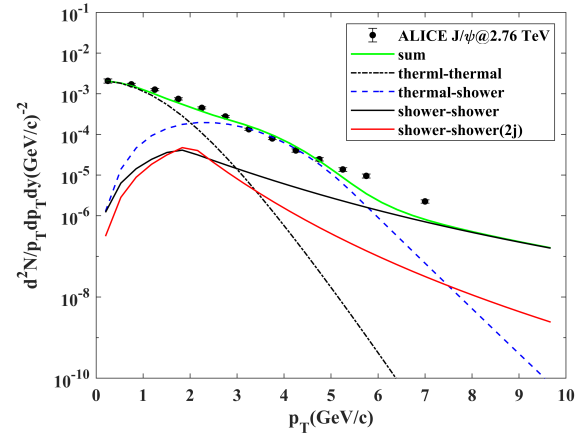


FIG. 20: J/ψ distribution at 2.76 TeV. $SS(2j)$: from 2 to 30 and from p to 30 when $p > 2$.

A. The issue for limit of integral in SS(2j)

The contribution of $SS(2j)$ in mediate p_T region seems too large. Therefore, we would like to do some tests for the limit of integral. Note that

$$\begin{aligned} \frac{dN_{J/\psi}^{SS(2)}}{pdः} &= \frac{10^{-n}}{p^0 p} \sum_{\substack{i=g,c \\ i'=g,c}} \int \frac{dq}{q} \frac{dq'}{q'} F_i'(q) F_{i'}'(q') \\ &\times S_i^c(\frac{p}{2q}) S_{i'}^c(\frac{p}{2q'}), \end{aligned} \quad (26)$$

First, we set up the integral region in the range of 2 to 30 GeV, and change the lower limit from 2 to p when $p = q$ to insure $\frac{p}{q} < 1$. Otherwise when $p > 2$ GeV, the lower

Then we change the lower limit from 2 to $p/2$ when $p/2 = q$ to insure $\frac{p}{2q} < 1$.

$$\begin{aligned} \frac{dN_{J/\psi}^{SS(2)}}{pdः} &= \frac{10^{-n}}{p^0 p} \int_2^{30} \int_2^{30} \sum_{\substack{i=g,c \\ i'=g,c}} \frac{dq}{q} \frac{dq'}{q'} F_i'(q) F_{i'}'(q') \\ &\times S_i^c(\frac{p}{2q}) S_{i'}^c(\frac{p}{2q'}) \end{aligned} \quad (29)$$

$$\begin{aligned} \downarrow \\ \downarrow \text{when } p > 4 \\ \downarrow \\ \frac{dN_{J/\psi}^{SS(2)}}{pdः} &= \frac{10^{-n}}{p^0 p} \int_{p/2}^{30} \int_{p/2}^{30} \sum_{\substack{i=g,c \\ i'=g,c}} \frac{dq}{q} \frac{dq'}{q'} F_i'(q) F_{i'}'(q') \\ &\times S_i^c(\frac{p}{2q}) S_{i'}^c(\frac{p}{2q'}) \end{aligned} \quad (30)$$

The results are shown in Fig.21.

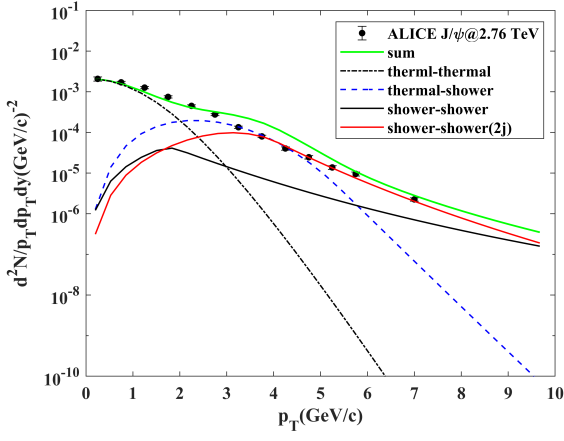


FIG. 21: J/ψ distribution at 2.76 TeV. $SS(2j)$: from 2 to 30 and from $p/2$ to 30 when $p > 4$.

To fit the data, we change the initial lower limit of integral from 2 to 3 and everything else remains the same.

$$\frac{dN_{J/\psi}^{SS(2)}}{pdः} = \frac{10^{-n}}{p^0 p} \int_3^{30} \int_3^{30} \sum_{\substack{i=g,c \\ i'=g,c}} \frac{dq}{q} \frac{dq'}{q'} F_i'(q) F_{i'}'(q') \times S_i^c(\frac{p}{2q}) S_{i'}^c(\frac{p}{2q'}) \quad (31)$$

↓

↓ when $p > 3$

↓

$$\frac{dN_{J/\psi}^{SS(2)}}{pdः} = \frac{10^{-n}}{p^0 p} \int_p^{30} \int_p^{30} \sum_{\substack{i=g,c \\ i'=g,c}} \frac{dq}{q} \frac{dq'}{q'} F_i'(q) F_{i'}'(q') \times S_i^c(\frac{p}{2q}) S_{i'}^c(\frac{p}{2q'}) \quad (32)$$

The results are shown in Fig.22.

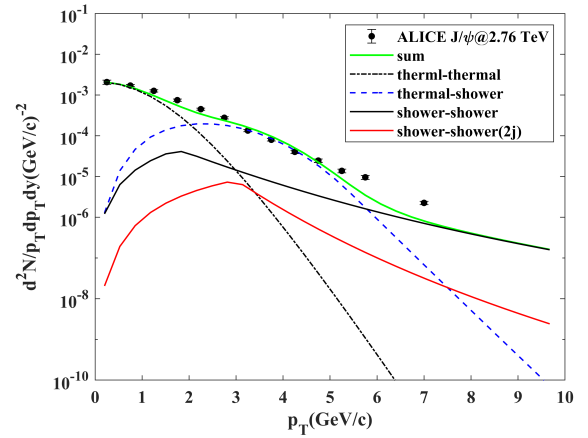


FIG. 22: J/ψ distribution at 2.76 TeV. $SS(2j)$: from 3 to 30 and from $p/2$ to 30 when $p > 2$.

Then we change the lower limit from 3 to $p/2$ when $p/2 = q$ to insure $\frac{p}{2q} < 1$.

$$\frac{dN_{J/\psi}^{SS(2)}}{pdः} = \frac{10^{-n}}{p^0 p} \int_{p/2}^{30} \int_{p/2}^{30} \sum_{\substack{i=g,c \\ i'=g,c}} \frac{dq}{q} \frac{dq'}{q'} F_i'(q) F_{i'}'(q') \times S_i^c(\frac{p}{2q}) S_{i'}^c(\frac{p}{2q'}) \quad (33)$$

↓

↓ when $p > 6$

↓

$$\frac{dN_{J/\psi}^{SS(2)}}{pdः} = \frac{10^{-n}}{p^0 p} \int_{p/2}^{30} \int_{p/2}^{30} \sum_{\substack{i=g,c \\ i'=g,c}} \frac{dq}{q} \frac{dq'}{q'} F_i'(q) F_{i'}'(q') \times S_i^c(\frac{p}{2q}) S_{i'}^c(\frac{p}{2q'}) \quad (34)$$

The results are shown in Fig.23.

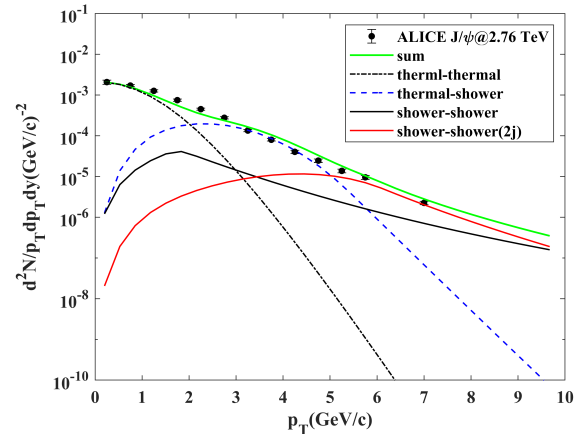


FIG. 23: J/ψ distribution at 2.76 TeV. $SS(2j)$: from 3 to 30 and from $p/2$ to 30 when $p > 6$.

All are listed above with $\Gamma = 10^{-2}$.

VII. MEETING 2022.11.07

We try to fit the distributions of charmed mesons with improved approaches above. The best results by fitting are shown in this section. And all the parameters used are listed here:

2.76 TeV :

$$T = 0.185 \text{ GeV}, \Gamma = 10^{-2}, \\ \gamma_l = 1.0, \gamma_s = 0.8, \gamma_c = 0.26$$

$$J/\psi : v_T = 0.25c, \quad (35)$$

$\beta L \rightarrow 0$ for charm, 2.39 for gluon

$$D^0 : v_T = 0.43c, \beta L = 5.8 \text{ for all} \quad (36)$$

$$D_s : v_T = 0.3c, \beta L = 4.0 \text{ for all.} \quad (37)$$

5.02 TeV :

$$T = 0.185 \text{ GeV}, \Gamma = 10^{-2}, \\ \gamma_l = 0.5, \gamma_s = 0.8, \gamma_c = 0.49$$

$$J/\psi : v_T = 0.28c, \quad (38)$$

$\beta L \rightarrow 0$ for charm, 2.39 for gluon

$$D^0 : v_T = 0.51c, \beta L = 5.8 \text{ for all} \quad (39)$$

$$D_s : v_T = 0.4c, \beta L = 4.0 \text{ for all.} \quad (40)$$

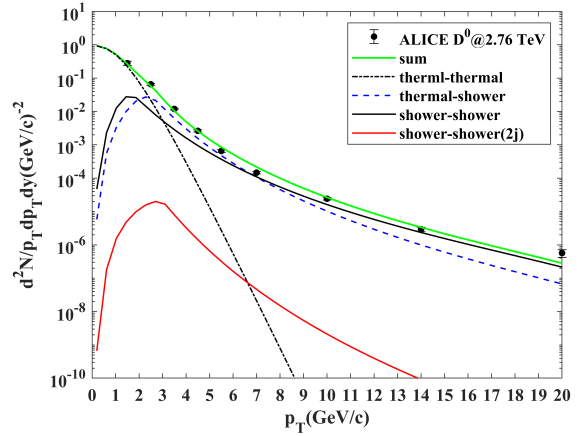


FIG. 25: D^0 distribution at 2.76 TeV.

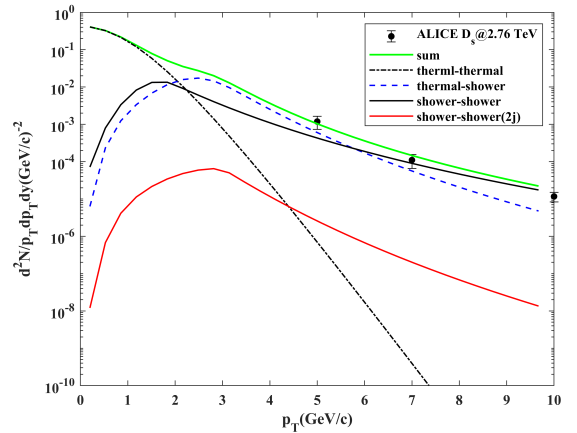


FIG. 26: D_s distribution at 2.76 TeV.

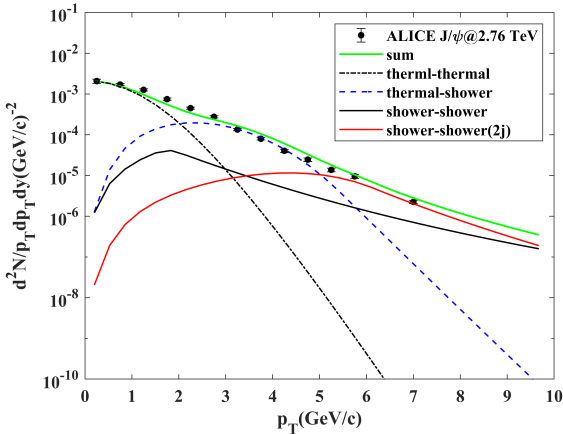


FIG. 24: J/ψ distribution at 2.76 TeV.

VIII. MEETING 2022.11.14

So far, two main issues have been put forward. One is that initial charm quark distribution $f_c(k)$ at 2.76 and 5.02 TeV should be determined reasonably. Prof. Min He has recommended FONLL Heavy Quark Production program (<http://www.lpthe.jussieu.fr/~cacciari/fonll/fonllform.html>) to produce charm distributions in pp collisions at any energy, which can figure out this issue.

We first get the factor, by which charm distribution multiplied or $(1/\pi) dsigma/dp_T^2/dy)$ divided, i.e. 3.2×10^6 at 5.5 TeV. Then the parameterized charm distribution

can be derived.

2.76 TeV:

$$\begin{aligned} f_c(p_T) &= \frac{dN_c}{d^2p_T} \\ &= \frac{\text{Exp}(20.406 - 3.343p_T^{0.5})}{3.2 \times 10^6} \end{aligned} \quad (41)$$

5.02 TeV:

$$\begin{aligned} f_c(p_T) &= \frac{dN_c}{d^2p_T} \\ &= \frac{\text{Exp}(20.49 - 3.15879p_T^{0.5})}{3.2 \times 10^6} \end{aligned} \quad (42)$$

The fitted results are shown in Fig.27.

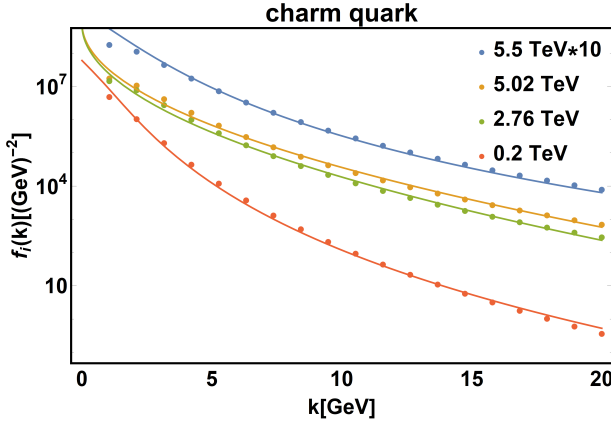


FIG. 27: Charm quark distributions $f_c(k)$ fitted by FONLL data.

Another is that which integral limits in terms of $SS(2j)$, described in Sec.VIA, should be adopted.

IX. MEETING 2022.11.28

Now new $f_c(k)$ is adopted to reproduce charmed mesons. And new fitted parameters are listed here:

2.76 TeV :

$$\begin{aligned} T &= 0.185 \text{ GeV}, \Gamma = 10^{-2}, \\ \gamma_l &= 1.0, \gamma_s = 0.8, \gamma_c = 0.26 \\ J/\psi &: v_T = 0.25c, \end{aligned} \quad (43)$$

$\beta L \rightarrow 0$ for charm, 2.39 for gluon

$$D^0 : v_T = 0.43c, \beta L = 3.5 \text{ for all}$$

$$D_s : v_T = 0.3c, \beta L = 2.9 \text{ for all.}$$

5.02 TeV :

$$T = 0.185 \text{ GeV}, \Gamma = 10^{-2},$$

$$\gamma_l = 0.5, \gamma_s = 0.3, \gamma_c = 0.49$$

$$J/\psi : v_T = 0.28c, \quad (44)$$

$\beta L \rightarrow 0$ for charm, 0.8 for gluon

$$D^0 : v_T = 0.51c, \beta L = 3.0 \text{ for charm, 7.0 for gluon}$$

$$D_s : v_T = 0.2c, \beta L = 2.0 \text{ for charm, 6.0 for gluon.}$$

Through those above, the spectra are shown below.

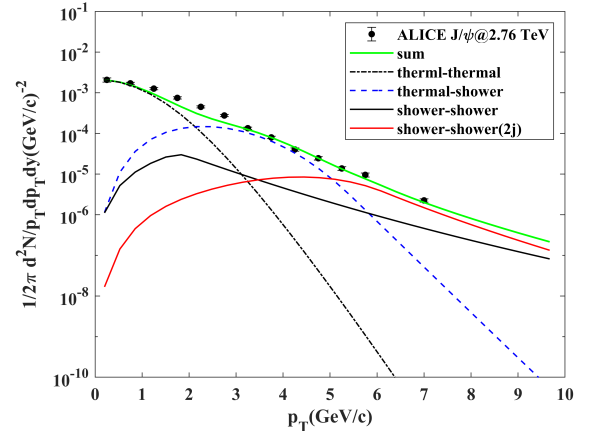


FIG. 28: J/ψ distribution at 2.76 TeV.

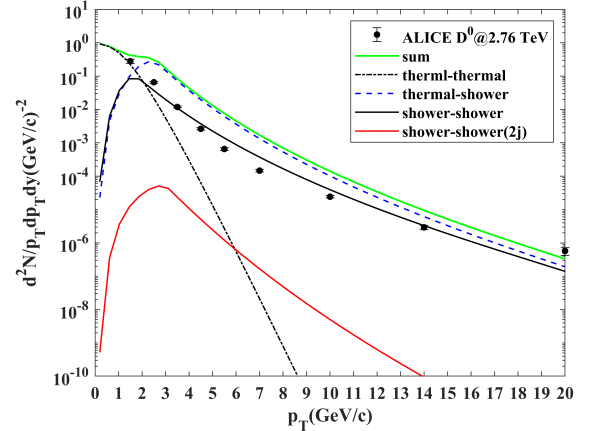


FIG. 29: D^0 distribution at 2.76 TeV.

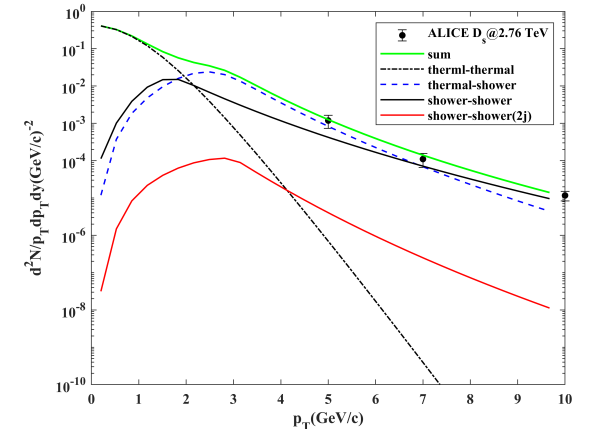
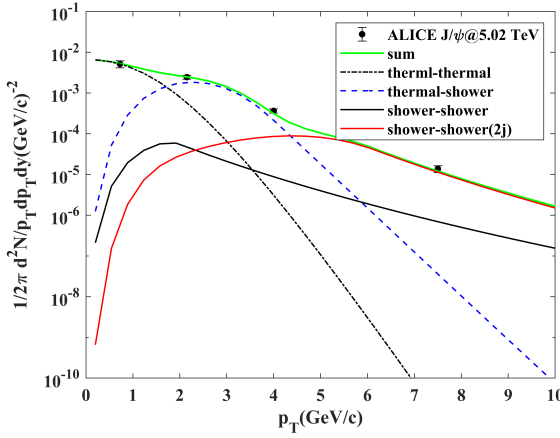
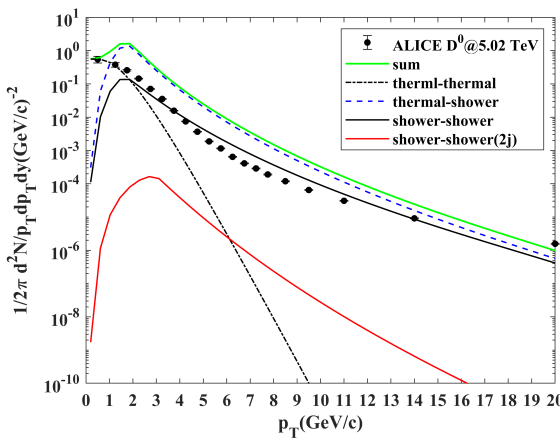
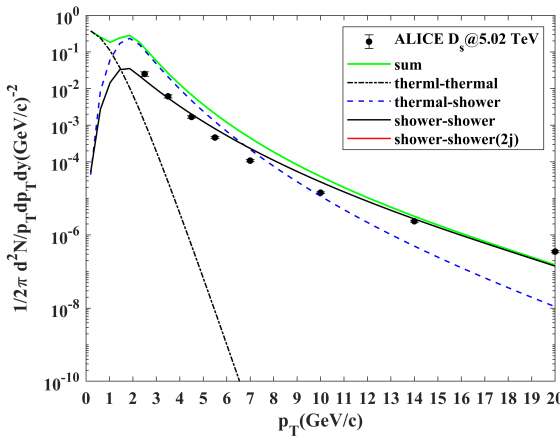


FIG. 30: D_s distribution at 2.76 TeV.

FIG. 31: J/ψ distribution at 5.02 TeV.FIG. 32: D^0 distribution at 5.02 TeV.FIG. 33: D_s distribution at 5.02 TeV.

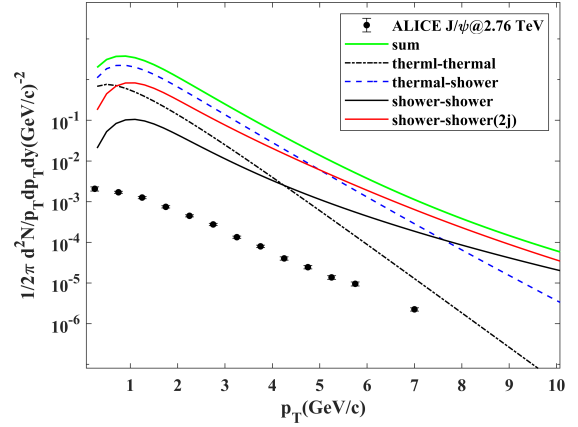
Next, we will check whether initial charm quark distribution is normalized and use `recomb_product_v15.f90`

to compare with last results to figure out SS(2j) integral issues.

X. MEETING 2022.12.05

Last week, by integration, we have found initial charm quark distribution is not normalized, so that the factor 3.2×10^6 is multiplied by direct. And the results using `recomb_product_v15.f90` are shown in Fig.34.

To calculate J/ψ by changing phi program: `p0:m(Jpsi)=3.096`, `fik:index 67` are note changed, however, `fik` has been changed. Questions: `gbst=0.432`? `Cs? C? T? Ts?` anything else not changed.

FIG. 34: J/ψ distribution at 2.76 TeV using `recomb_product_v15.f90`.

Then, due to various framework compared with recombination model, we only adopt $SS(2j)$ in version15 program.

XI. MEETING 2022.12.12

This week, first, considering inconsistent asymptotic behavior of charm jet distribution at low momentum, its contribution is cut off by a smooth function, like Fermi-Dirac distribution, which we take to be [13] for gluon

$$g(q) = [1 + e^{(3.5-q)/0.5}]^{-1}. \quad (45)$$

Similarly, charm jet distributions can be given below, shown in 35.

2.76 TeV:

$$\begin{aligned} f_c(p_T) &= \frac{dN_c}{d^2p_T} \\ &= \frac{\text{Exp}(20.406 - 3.343p_T^{0.5})}{3.5 \times 10^6} \\ &\times \frac{1}{1 + e^{\frac{0.84 - p_T}{0.257}}} \end{aligned} \quad (46)$$

5.02 TeV:

$$\begin{aligned} f_c(p_T) &= \frac{dN_c}{d^2p_T} \\ &= \frac{\text{Exp}(20.49 - 3.15879p_T^{0.5})}{3.5 \times 10^6} \\ &\times \frac{1}{1 + e^{\frac{1.05 - p_T}{0.3}}} \end{aligned} \quad (47)$$

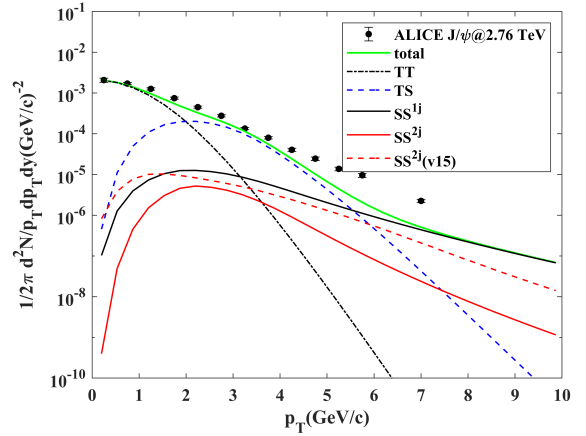


FIG. 36: J/ψ distribution at 2.76 TeV.

I should check $SS(1)$ to fit data and $SS(2)$ summing over charm and gluon, while v15 summing over light quark, gluon and charm.

XII. MEETING 2022.12.19

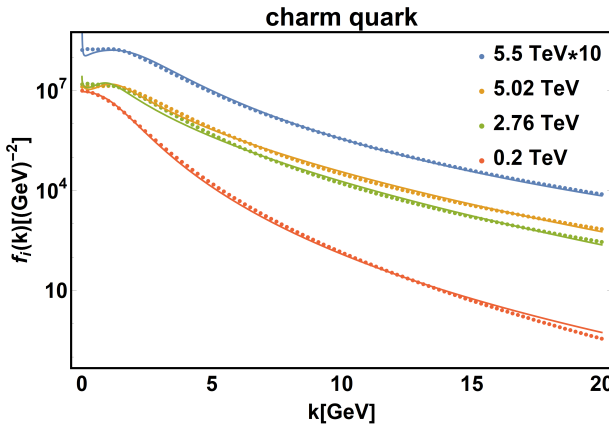


FIG. 35: Charm quark distributions $f_c(k)$ fitted by FONLL data.

Besides, compared with v15 $SS(2j)$ component:

$$\frac{dN_{J/\psi}^{SS^{2j}}}{p_T dp_T} = \frac{g\Gamma}{p_T m_T^{J/\psi}} S^c(p_T/2) S^{\bar{c}}(p_T/2), \quad (48)$$

our integral limit in Eq.30 actually is consistent with it. After adding QuenchFiqc 45 and QuenchSPD 49 from v15 to our program, we calculated distributions again shown in Fig.36.

$$c_2(p_2) = 1 - e^{-(p_2/p_c)^2}, p_c = 0.5 \text{ GeV}/c. \quad (49)$$

Last week, as for $SS(2)$ issues, it is found that the difference between two frameworks is minijet distributions. In our(R. Peng) framework, it is easy to write

$$\begin{aligned} \frac{dN_{J/\psi}^{SS(2)}}{pd^2p} &= \frac{10^{-n}}{p^0 p} \sum_{\substack{i=g,c \\ i'=g,c}} \int \frac{dq}{q} \frac{dq'}{q'} F'_i(q) F'_{i'}(q') \\ &\times S_i^{\bar{c}}\left(\frac{p}{2q}\right) S_{i'}^c\left(\frac{p}{2q'}\right), \end{aligned} \quad (50)$$

$$F'_i(q) = \frac{1}{\beta L} \int_q^{qe^{\beta L}} dk k f_i(k). \quad (51)$$

However, in previous RM framework[3], considering azimuthal angle ϕ and impact parameter b , much more complex formula is written as

$$F'_i(q) = \int d\xi P_i(\xi, \phi, b) \int dk k f_i(k) G(k, q, \xi), \quad (52)$$

$$G(k, q, \xi) = q\delta(q - ke^{-\xi}), \quad (53)$$

$$\gamma_g(g) = \frac{\gamma_0}{1 + (q/q_0)^2}, \quad (54)$$

$$\gamma_0 = 2.8, q_0 = 7, \text{ PbPb@2.76}. \quad (55)$$

Thus, in two framework, there are parameters γ_0 , q_0 or βL to fit respectively. It is difficult to compare them owing to no right reference. While transferring code from v15 to ours, it is verified that shower parton distribution S_i^j is much larger than ours. Next we determine $SS(1)$ first to ensure minijet distribution, in which v15 used different method for calculation.

As a result, calculation of $SS(2)$ adopted process in v15, except for S_i^j . All are shown in Fig.37.

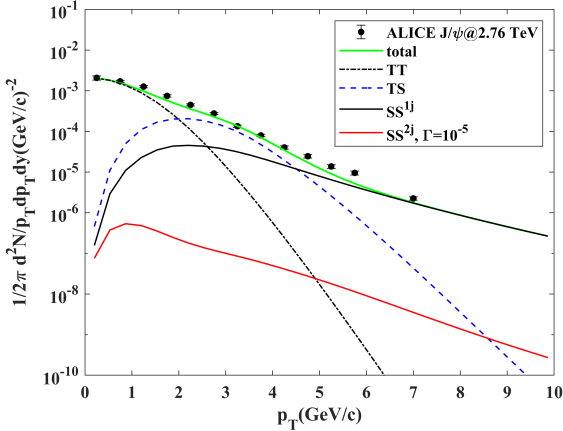


FIG. 37: J/ψ distribution at 2.76 TeV.

We should figure out the bug in calculation of $SS(2)$.

XIII. MEETING 2023.01.02

Last week, the bug in $SS(2)$ was found, which is a wrong order in a loop, resulting in much larger results in $SS(2)$. After modifying, new spectrum is shown in Fig.38.

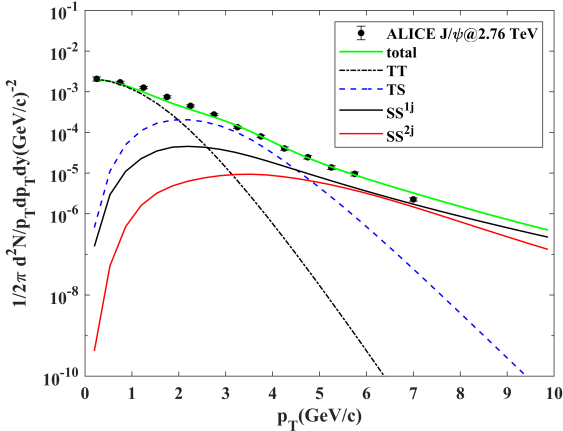


FIG. 38: J/ψ distribution at 2.76 TeV with $\Gamma = 10^{-2}$.

Next, I will check all the code and reproduce others.

XIV. MEETING 2023.01.09

After refactoring the code, the first results are shown below. And next parameters should be fitted to be consistent with experiments.

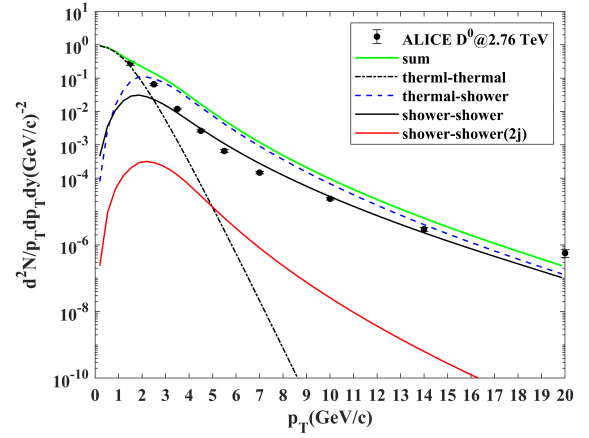


FIG. 39: D^0 distribution at 2.76 TeV with $\Gamma = 10^{-2}$.

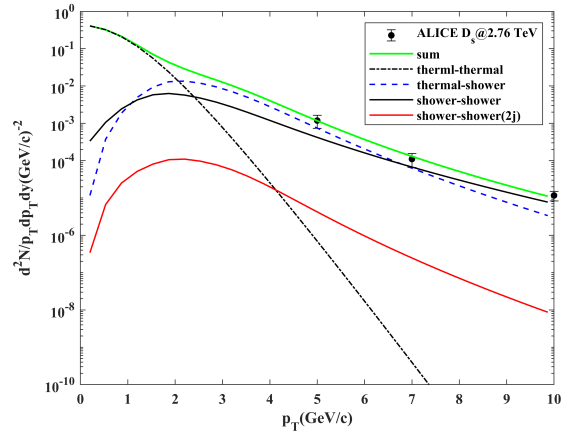


FIG. 40: D_s distribution at 2.76 TeV with $\Gamma = 10^{-2}$.

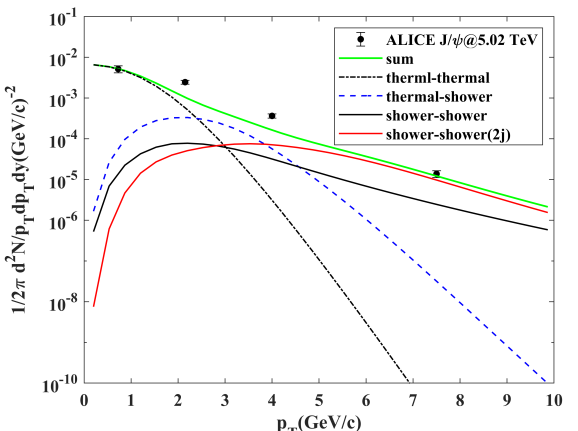


FIG. 41: J/ψ distribution at 5.02 TeV with $\Gamma = 10^{-2}$.

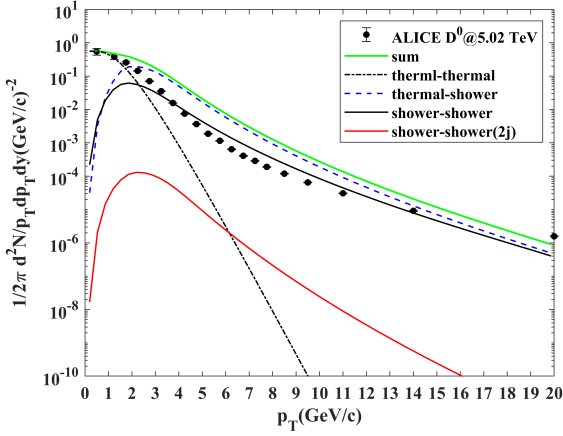
XVI. MEETING 2023.02.06


FIG. 42: D^0 distribution at 5.02 TeV with $\Gamma = 10^{-2}$.

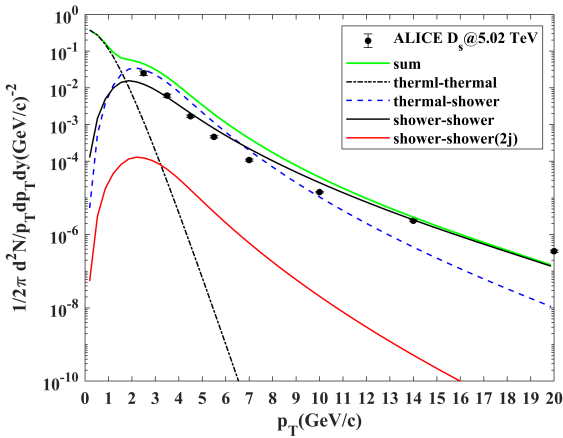


FIG. 43: D_s distribution at 5.02 TeV with $\Gamma = 10^{-2}$.

It is suggested that we should replace all the integral algorithm with exponential integral algorithm in v15 program, owing to the scale of integrand.

XV. MEETING 2023.01.30

While adding exponential integral algorithm in v15 program, we find it difficult to reproduce spectrum using old parameters in v15 (the step fdel=0.02, 0.05, 0.1). Thus this issue is tackled after decreasing the step to 0.01/0.005, however, increasing the computing cost, so that now we can reproduce spectrum for J/ψ and D^0 at 2.76 TeV at least.

It is suggested to check the accuracy of integral algorithms. Then we will fit the spectrum.

After checking the accuracy of integral algorithms, it is found that the step 0.01 is suitable for our calculation. Then we fit the spectrum, shown below.

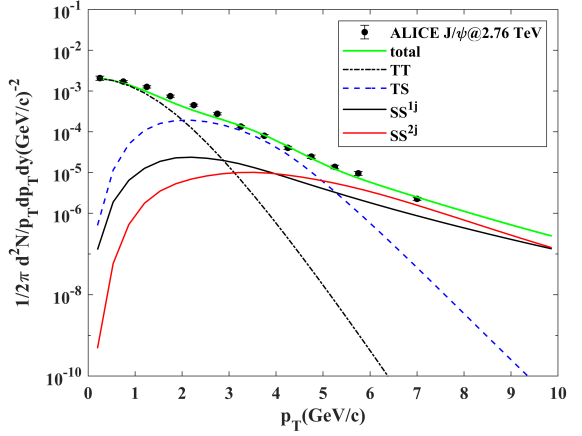


FIG. 44: J/ψ distribution at 2.76 TeV with $\Gamma = 10^{-2}$.

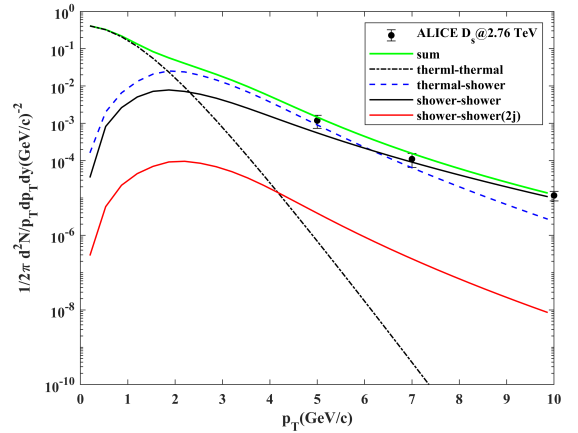
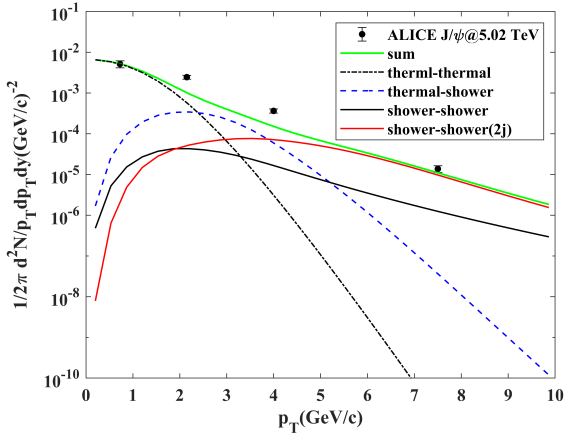
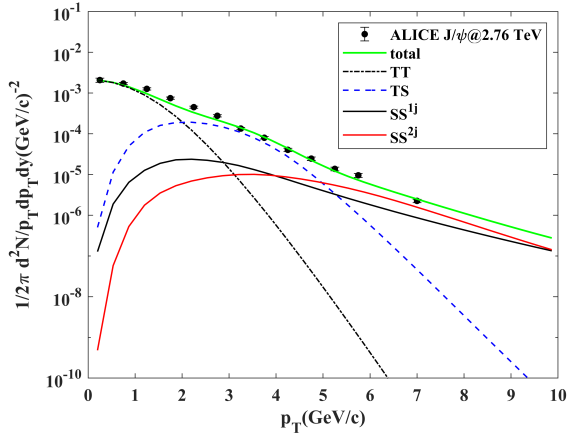


FIG. 45: D_s distribution at 2.76 TeV with $\Gamma = 10^{-2}$.

FIG. 46: J/ψ distribution at 5.02 TeV with $\Gamma = 10^{-2}$.FIG. 47: J/ψ distribution at 2.76 TeV with $\Gamma = 10^{-2}$.

It is suggested to fix the step size at 0.05 to fit parameters and then turn it down as we need.

XVII. MEETING 2023.02.13

Latest fitted parameters are listed here:

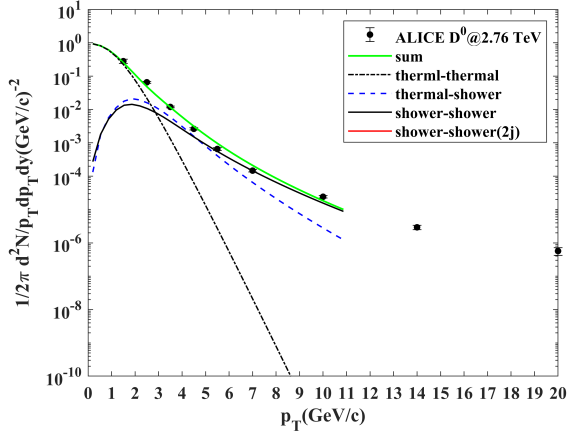
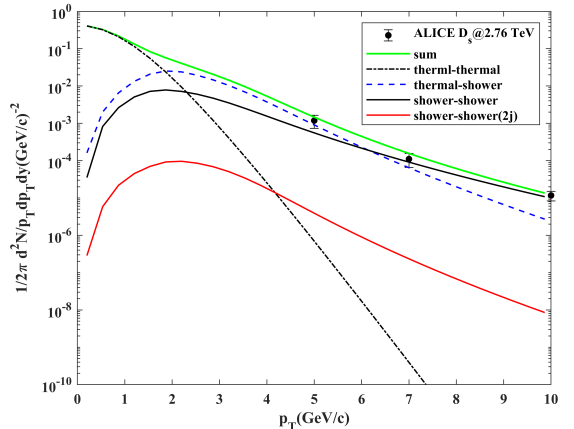
2.76 TeV :

$$\begin{aligned} T &= 0.185 \text{ GeV}, \Gamma = 10^{-2}, \\ \gamma_l &= 1.0, \gamma_s = 0.8, \gamma_c = 0.26 \\ J/\psi : v_T &= 0.25c, \quad (56) \\ \beta L &\rightarrow 0 \text{ for charm, } 2.39 \text{ for gluon} \\ D^0 : v_T &= 0.43c, \beta L = 8.0 \text{ for all} \\ D_s : v_T &= 0.3c, \beta L = 2.39 \text{ for all.} \end{aligned}$$

5.02 TeV :

$$\begin{aligned} \Gamma &= 10^{-2}, \\ \gamma_l &= 1.0, \gamma_s = 0.8, \gamma_c = 0.39 \\ J/\psi : v_T &= 0.25c, T = 0.190 \text{ GeV}, \quad (57) \\ \beta L &\rightarrow 0 \text{ for charm, } 0.1 \text{ for gluon} \\ D^0 : v_T &= 0.5c, T = 0.175 \text{ GeV}, \quad (58) \\ \beta L &= 3.0 \text{ for charm, } 7.0 \text{ for gluon} \\ D_s : v_T &= 0.3c, T = 0.175 \text{ GeV}, \quad (59) \\ \beta L &= 2.0 \text{ for charm, } 6.0 \text{ for gluon.} \end{aligned}$$

Through those above, the spectra are shown below. We have improved the spectra of D^0 at 2.76 TeV. Note that TS component in Fig.48 should have been larger than what we see, because TS component is calculated by using step 0.05 for triple integral.

FIG. 48: D^0 distribution at 2.76 TeV with $\Gamma = 10^{-2}$.FIG. 49: D_s distribution at 2.76 TeV with $\Gamma = 10^{-2}$.

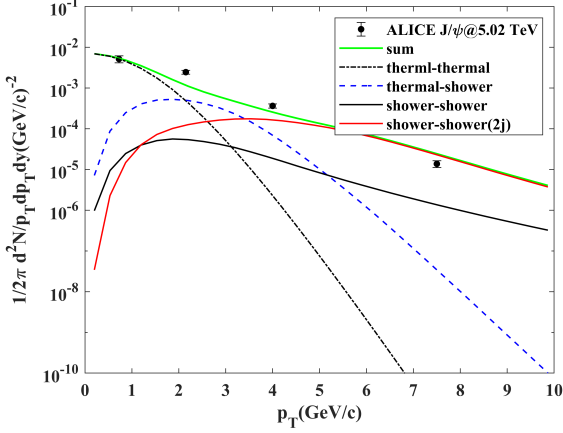
XVIII. MEETING 2023.02.20


FIG. 50: J/ψ distribution at 5.02 TeV with $\Gamma = 10^{-2}$.

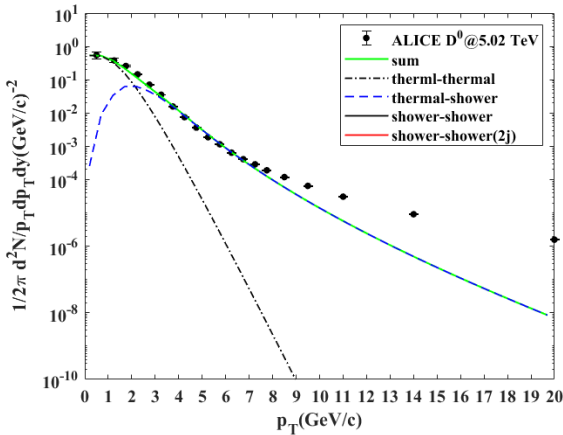


FIG. 51: D^0 distribution at 5.02 TeV with $\Gamma = 10^{-2}$.

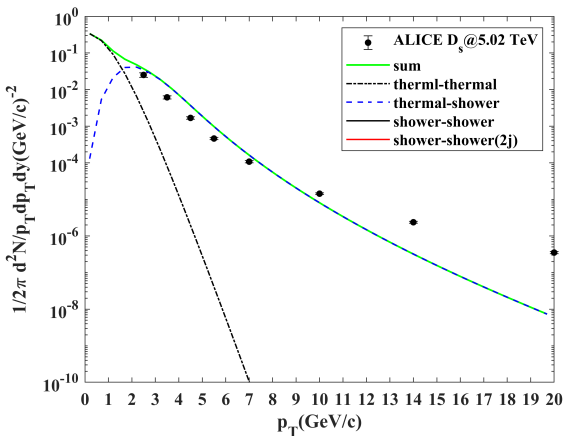


FIG. 52: D_s distribution at 5.02 TeV with $\Gamma = 10^{-2}$.

Since last week, we decline the number of calculated points and fix the first point at $p_T = 0.5$ GeV/c owing to uncertain validity for RM at such a low transverse momentum. And before, it is checked that the accuracy of single exponential integral algorithm is suitable(4 significant figures) for our calculation, when the step fdel=0.05. However, for triple exponential integral algorithm, it can be obtained only one significant figure when the step fdel=0.02 and two significant figures when the step fdel=0.01. To derive accurate results with lower computational cost, we choose the step fdel=0.02 finally. Note that the abnormal phenomenon only appeared in the spectra of D^0 , that the contribution from $SS(1)$ exceeds that from TS at the first point, has vanished after changing the first point and improving accuracy.

Latest fitted parameters and spectra are listed here:

2.76 TeV :

$$\begin{aligned} T &= 0.185 \text{ GeV}, \Gamma = 10^{-2}, \\ \gamma_l &= 1.0, \gamma_s = 0.8, \gamma_c = 0.26 \\ J/\psi &: v_T = 0.25c, \quad (60) \\ \beta L &\rightarrow 0 \text{ for charm, } 2.39 \text{ for gluon} \\ D^0 &: v_T = 0.43c, \beta L = 8.0 \text{ for all} \\ D_s &: v_T = 0.3c, \beta L = 2.39 \text{ for all.} \end{aligned}$$

5.02 TeV :

$$\begin{aligned} \Gamma &= 10^{-2}, \\ \gamma_l &= 1.0, \gamma_s = 0.8, \gamma_c = 0.39 \\ J/\psi &: v_T = 0.25c, T = 0.190 \text{ GeV}, \quad (61) \\ \beta L &\rightarrow 0 \text{ for charm, } 0.1 \text{ for gluon} \\ D^0 &: v_T = 0.5c, T = 0.175 \text{ GeV}, \quad (62) \\ \beta L &= 8.0 \text{ for charm and gluon, } 5.0 \text{ for } \bar{s} \\ D_s &: v_T = 0.3c, T = 0.175 \text{ GeV}, \quad (63) \\ \beta L &= 7.0 \text{ for charm and gluon, } 5.0 \text{ for } \bar{s}. \end{aligned}$$

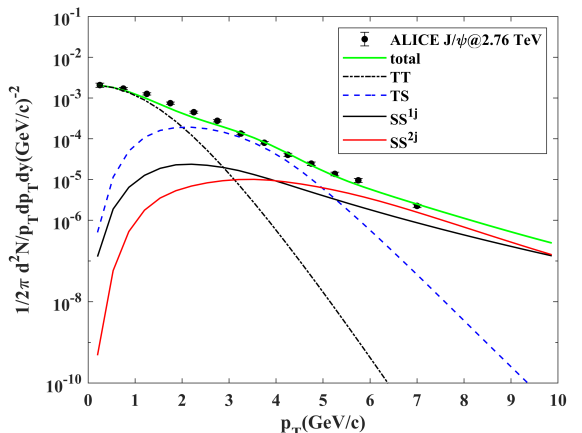
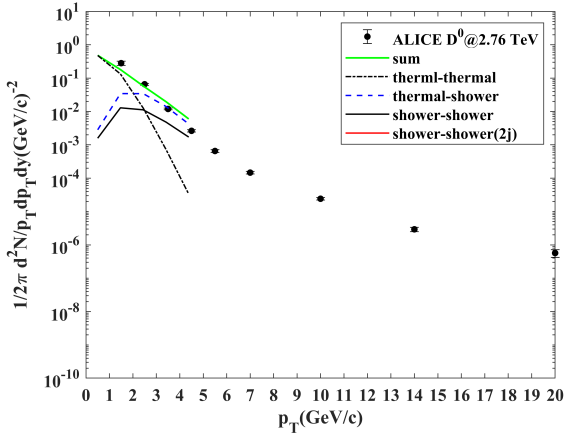
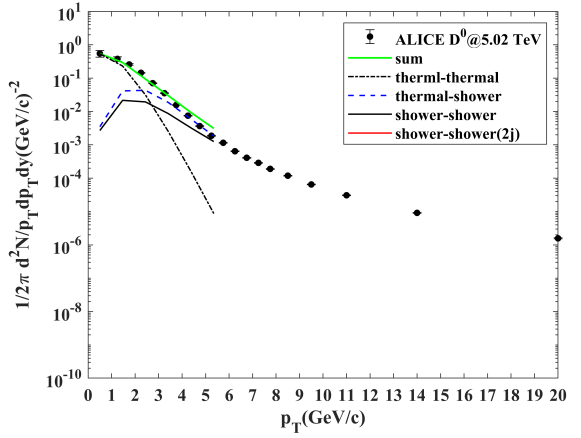
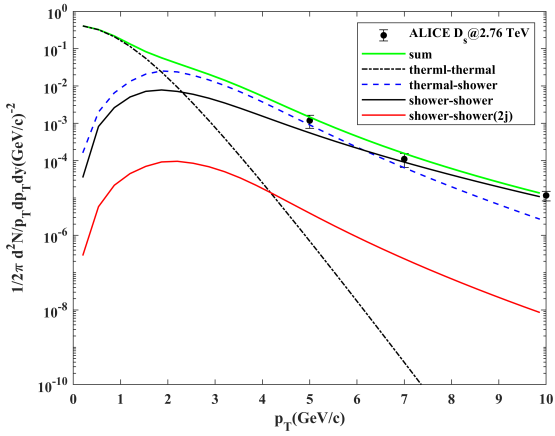
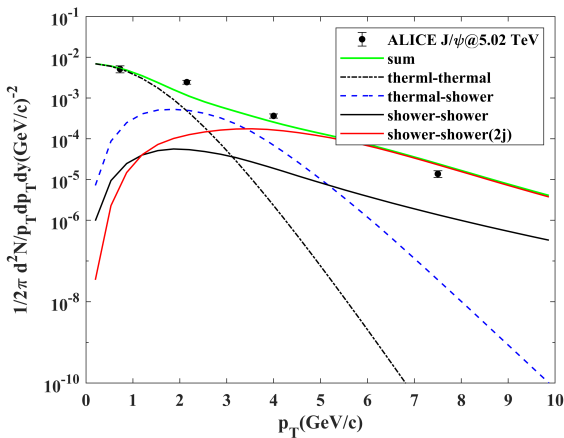
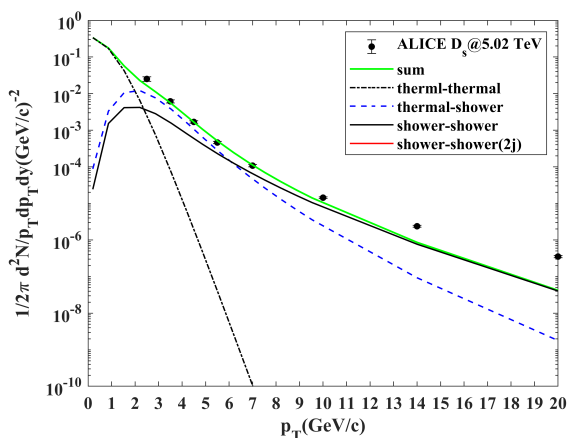


FIG. 53: J/ψ distribution at 2.76 TeV with $\Gamma = 10^{-2}$.

FIG. 54: D^0 distribution at 2.76 TeV with $\Gamma = 10^{-2}$.FIG. 57: D^0 distribution at 5.02 TeV with $\Gamma = 10^{-2}$.FIG. 55: D_s distribution at 2.76 TeV with $\Gamma = 10^{-2}$.FIG. 56: J/ψ distribution at 5.02 TeV with $\Gamma = 10^{-2}$.FIG. 58: D_s distribution at 5.02 TeV with $\Gamma = 10^{-2}$.

XIX. MEETING 2023.02.27

Latest fitted parameters and spectra are listed here:

2.76 TeV :

$$T = 0.185 \text{ GeV}, \Gamma = 10^{-2},$$

$$\gamma_l = 1.0, \gamma_s = 0.8, \gamma_c = 0.26$$

$$J/\psi : v_T = 0.25c, \quad (64)$$

$\beta L \rightarrow 0$ for charm, 2.39 for gluon

$$D^0 : v_T = 0.43c, \beta L = 17.0 \text{ for all}$$

$$D_s : v_T = 0.3c, \beta L = 2.9 \text{ for all.}$$

5.02 TeV :

$$\Gamma = 10^{-2},$$

$$\gamma_l = 1.0, \gamma_s = 0.8, \gamma_c = 0.39$$

$$J/\psi : v_T = 0.25c, T = 0.190 \text{ GeV}, \quad (65)$$

$\beta L \rightarrow 0$ for charm, 0.1 for gluon

$$D^0 : v_T = 0.5c, T = 0.175 \text{ GeV}, \quad (66)$$

$\beta L = 17.0 \text{ for all}$

$$D_s : v_T = 0.3c, T = 0.175 \text{ GeV}, \quad (67)$$

$\beta L = 7.0 \text{ for charm and gluon, 5.0 for } \bar{s}$.

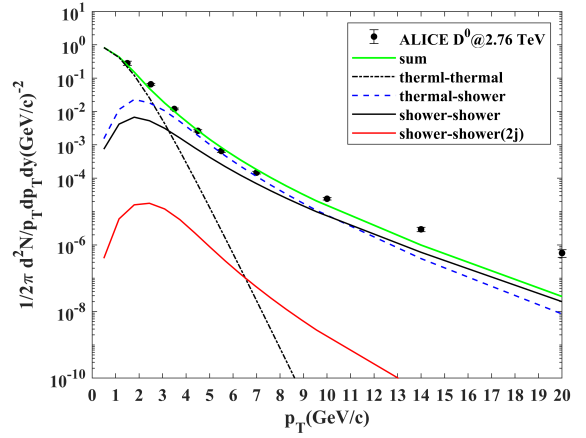


FIG. 60: D^0 distribution at 2.76 TeV with $\Gamma = 10^{-2}$.

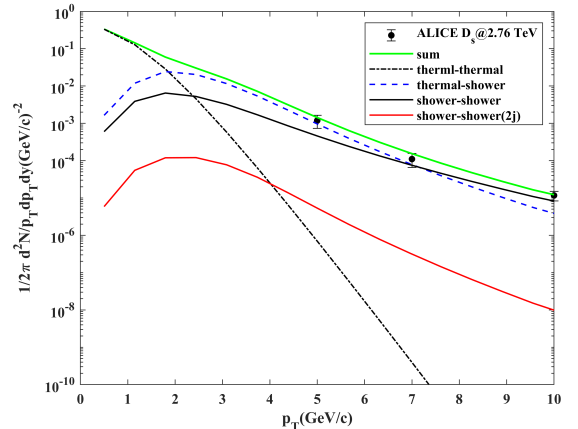


FIG. 61: D_s distribution at 2.76 TeV with $\Gamma = 10^{-2}$.

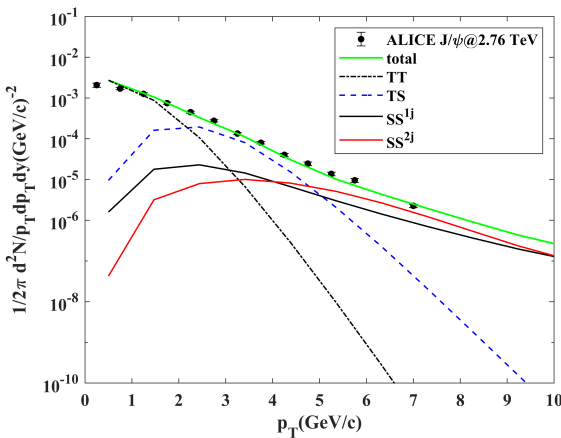


FIG. 59: J/ψ distribution at 2.76 TeV with $\Gamma = 10^{-2}$.

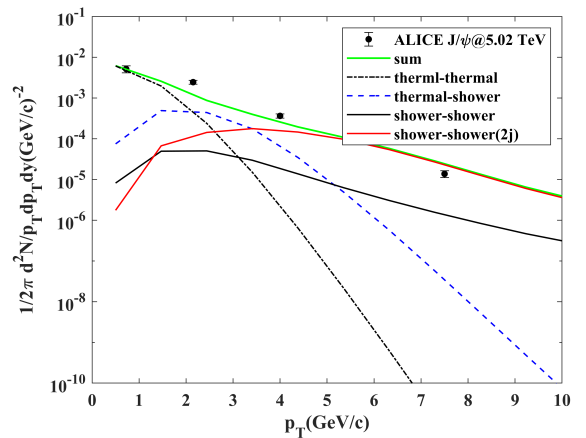
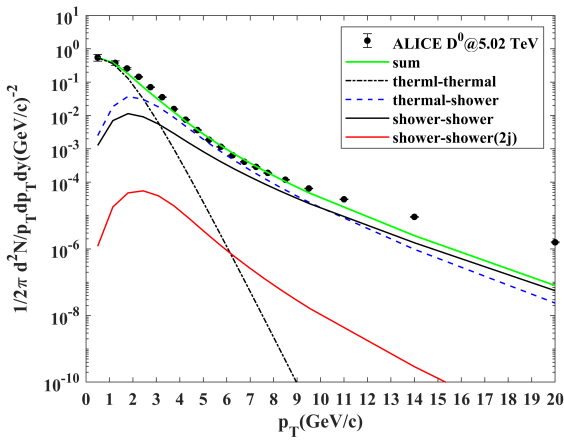
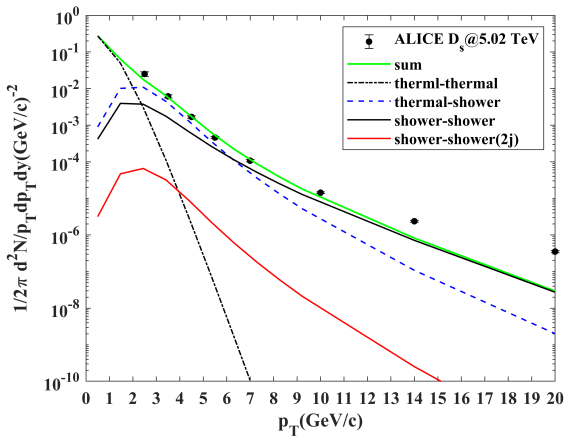
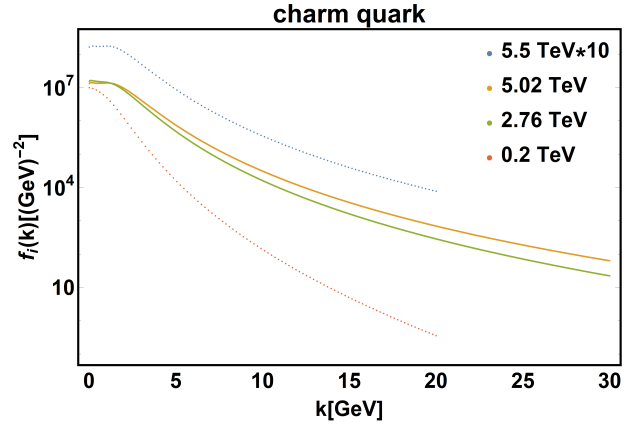


FIG. 62: J/ψ distribution at 5.02 TeV with $\Gamma = 10^{-2}$.

FIG. 63: D^0 distribution at 5.02 TeV with $\Gamma = 10^{-2}$.FIG. 64: D_s distribution at 5.02 TeV with $\Gamma = 10^{-2}$.FIG. 65: Charm jet distribution $f_c(k)$ produced by FONLL.

XX. MEETING 2023.03.05

In spite of agreement with experimental data, the fitted parameters seem unreasonable. Thus we will do some check in the followings.

First, all data are plotted in one figure below.

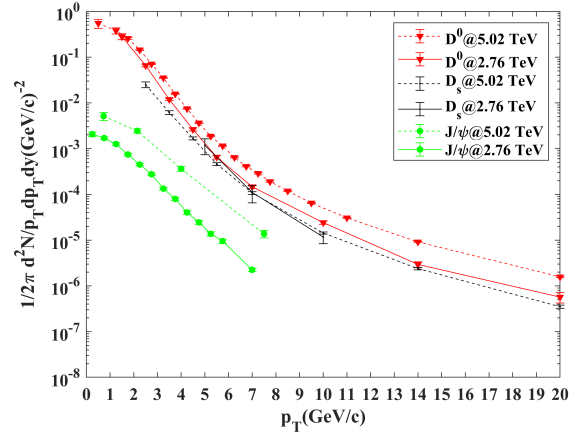


FIG. 66: Experimental data of three mesons at two energy.

Considering the unreliable fitted formula Eq.47 and Eq.47 in Fig.35 at large momentum, leading to generally inaccurate results at high p_T in spectra above, we directly produce 3000 points from FONLL shown in Fig.65 and read them in program, like the way of MatFicq.

Second, we check the spectrum of D^0 , replacing $F'_i(q)$ by $f_i(k)$. In practice, we just set $bL=0.01$, assuming the dynamic length tends to 0, i.e. no momentum decay at creation.

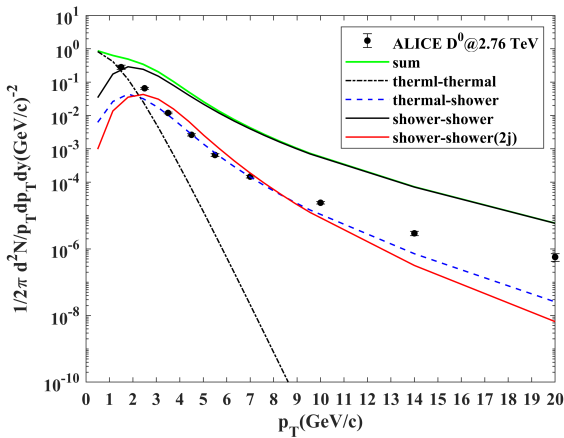


FIG. 67: D^0 distribution at 2.76 TeV with $\Gamma = 10^{-2}$ when $bL=0.01$.

Third, the thermal distribution at 2.76 and 5.02 TeV are fitted by $C * \exp(-p_T/T)$ respectively.

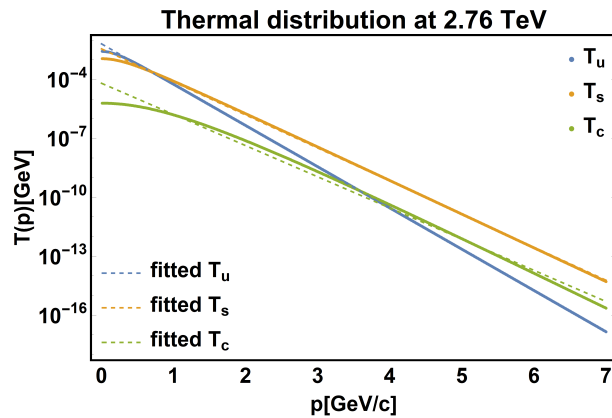


FIG. 68: Thermal parton distribution at 2.76 TeV.

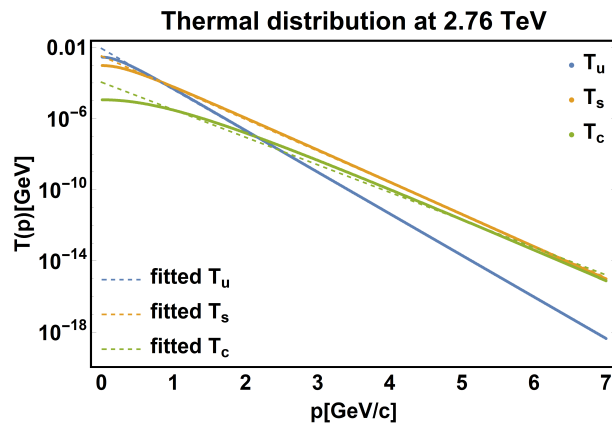


FIG. 69: Thermal parton distribution at 5.02 TeV.

Fourth, we reproduce the results at the beginning of this paper after debugging.

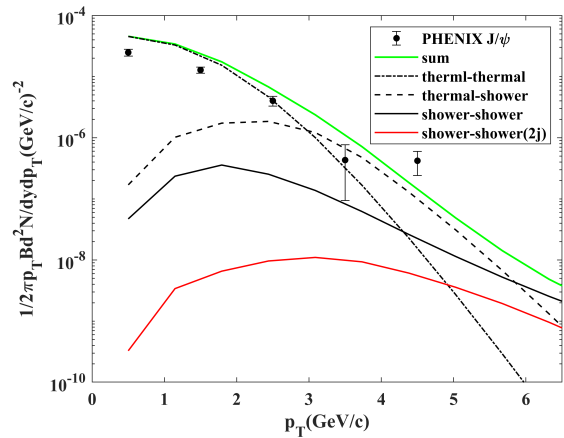


FIG. 70: J/ψ distribution at 200 GeV with $\Gamma = 10^{-2}$.

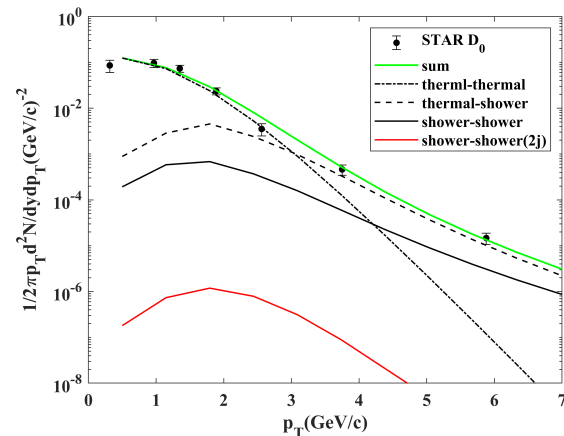


FIG. 71: D^0 distribution at 200 GeV with $\Gamma = 10^{-2}$.

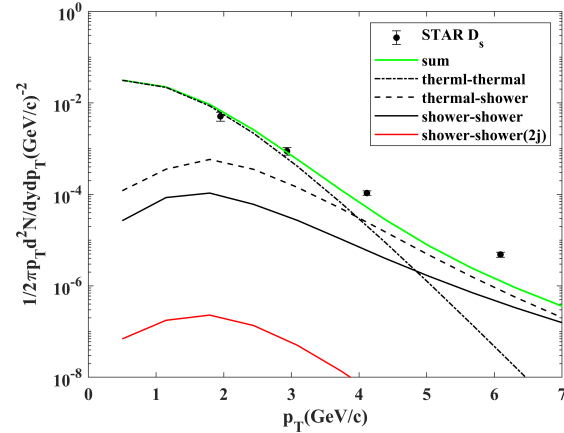


FIG. 72: D_s distribution at 200 GeV with $\Gamma = 10^{-2}$.

XXI. MEETING 2023.03.13

Last week, we figured out the importance of cutoff in shower, the same as v15(2~30). Then it is corrected to 3~30, shown better agreement below.

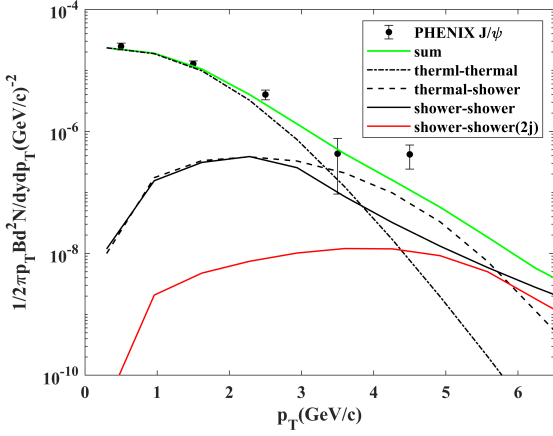


FIG. 73: J/ψ distribution at 200 GeV with $\Gamma = 10^{-2}$, $q = 3 \sim 30$.

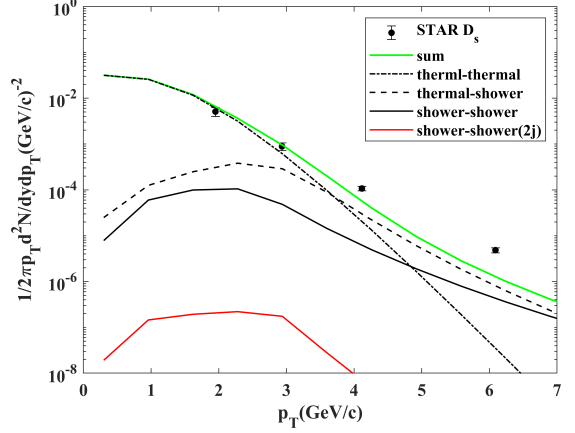


FIG. 75: D_s distribution at 200 GeV with $\Gamma = 10^{-2}$, $q = 3 \sim 30$.

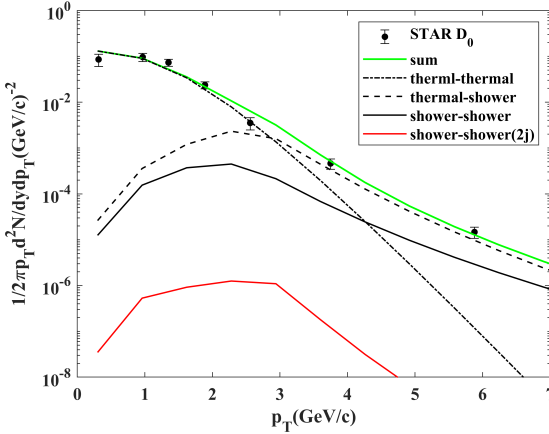


FIG. 74: D^0 distribution at 200 GeV with $\Gamma = 10^{-2}$, $q = 3 \sim 30$.

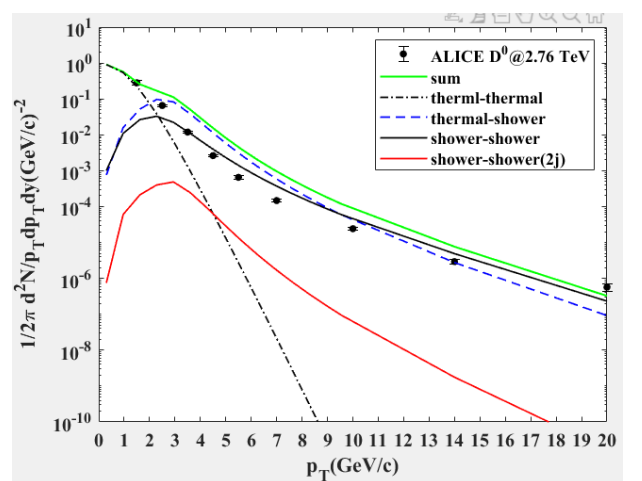


FIG. 76: D^0 distribution at 2.76 TeV with $\Gamma = 10^{-2}$, $q = 3 \sim 30$, $bL = 2.9$.

Thus, we attempt to utilize it to correct the strangeness of parameters for D^0 . Through a lot of tests below, it seems hard to correct bL from 17.0 to 2.9. In Fig.81, $bL = 15.0$ and $q = 3 \sim 30$ was used and a little improvement was seen.

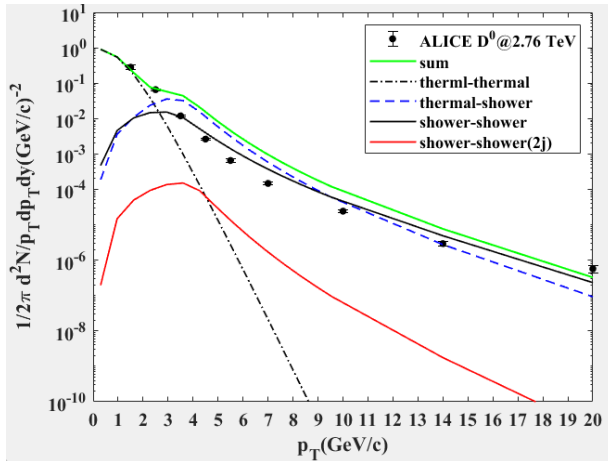


FIG. 77: D^0 distribution at 2.76 TeV with $\Gamma = 10^{-2}$, $q = 4 \sim 30$, $bL = 2.9$.

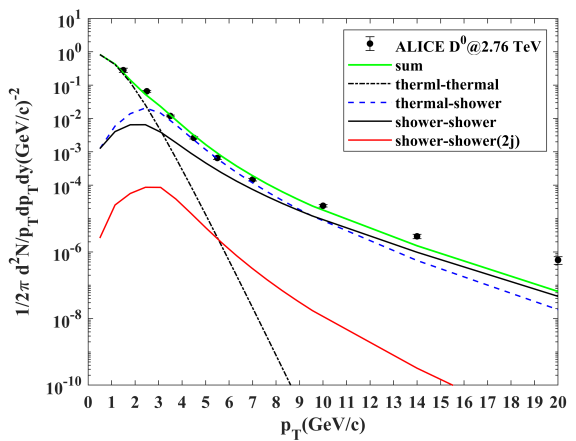


FIG. 81: D^0 distribution at 2.76 TeV with $\Gamma = 10^{-2}$, $q = 3 \sim 30$, $bL = 15$.

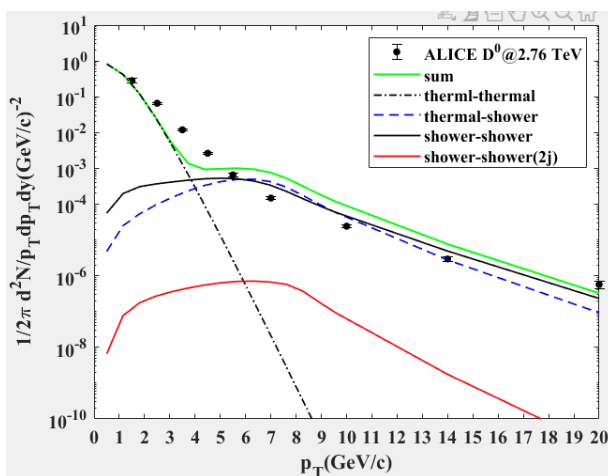


FIG. 78: D^0 distribution at 2.76 TeV with $\Gamma = 10^{-2}$, $q = 8 \sim 30$, $bL = 2.9$.

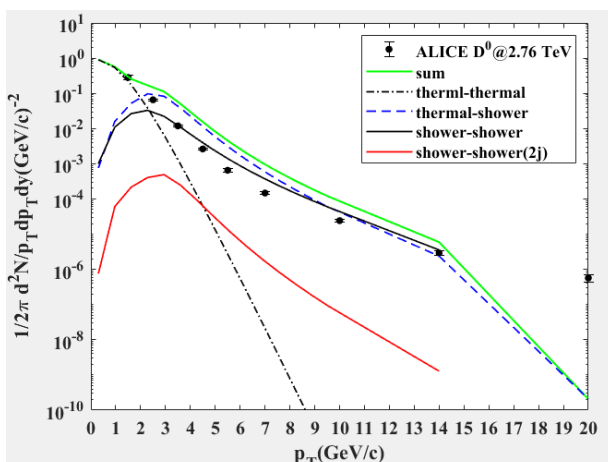
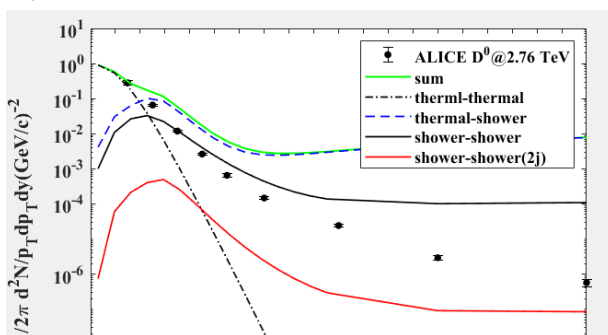


FIG. 79: D^0 distribution at 2.76 TeV with $\Gamma = 10^{-2}$, $q = 3 \sim 20$, $bL = 2.9$.



XXII. MEETING 2023.04.10

Parameters should be modified in v16:

$$T_c, C_c, \gamma_0, q_0, gbst \quad (68)$$

Question: am, bm in subroutine *meson_coe*, function FF(IDH, IDparticle, x)

XXIII. MEETING 2023.05.29

Since parameters of previous program are unreasonable, we move to v16 constructed from v15. We find that recombination function in [3](JPG) is different from [11, 14, 15](R. P.), which mainly reflected in whether it includes the parameter g_M . We will use the former in v16, including g_M . And then the formulae of mesons are given here,

$$\frac{dN_{D^0}^{TT}}{d^2p} = \frac{5g_{D^0}C_qC_c}{p_0 p_T^6} \int_0^{p_T} dp_1 p_1 e^{-p_1/T_q} (p_T - p_1) e^{-(p_T - p_1)/T_c} (p_T - p_1)^4, \quad (69)$$

$$\frac{dN_{D^0}^{TS}}{d^2p} = \frac{5g_{D^0}}{p_0 p_T^6} \int_0^{p_T} dp_1 p_1 (p_T - p_1)^4 [C_q e^{-p_1/T_q} S^c(p_T - p_1) + C_c (\frac{p_T}{p_1} - 1) e^{-(p_T - p_1)/T_c} S^{\bar{u}}(p_1)], \quad (70)$$

$$\frac{dN_{D_s}^{TT}}{d^2p} = \frac{660g_{D_s}C_sC_c}{p_0 p_T^{13}} \int_0^{p_T} dp_1 p_1 e^{-p_1/T_s} (p_T - p_1) e^{-(p_T - p_1)/T_c} p_1^2 (p_T - p_1)^9, \quad (71)$$

$$\frac{dN_{D_s}^{TS}}{d^2p} = \frac{660g_{D_s}}{p_0 p_T^{13}} \int_0^{p_T} dp_1 p_1^3 (p_T - p_1)^9 [C_s e^{-p_1/T_s} S^c(p_T - p_1) + C_c (\frac{p_T}{p_1} - 1) e^{-(p_T - p_1)/T_c} S^{\bar{s}}(p_1)]. \quad (72)$$

After fitting, parameters in I and results are listed here.

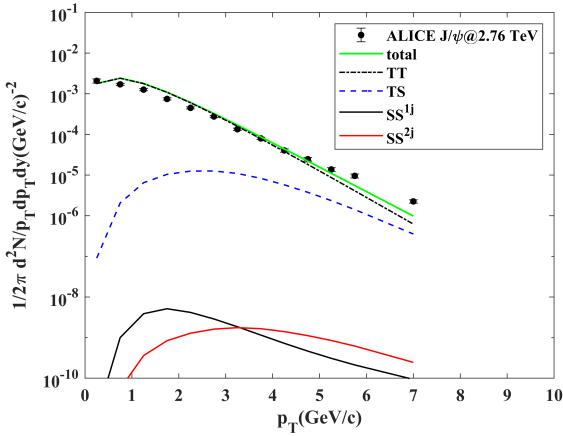


FIG. 82: J/ψ distribution at 2.76 TeV.

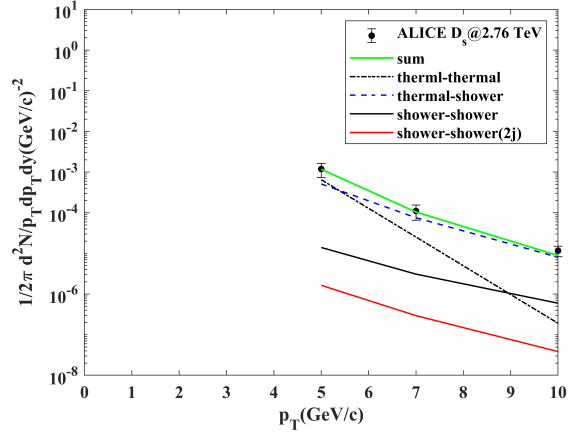


FIG. 84: D_s distribution at 2.76 TeV.

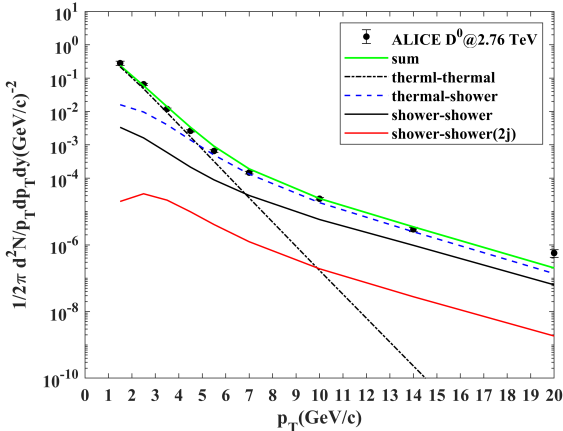


FIG. 83: D^0 distribution at 2.76 TeV.

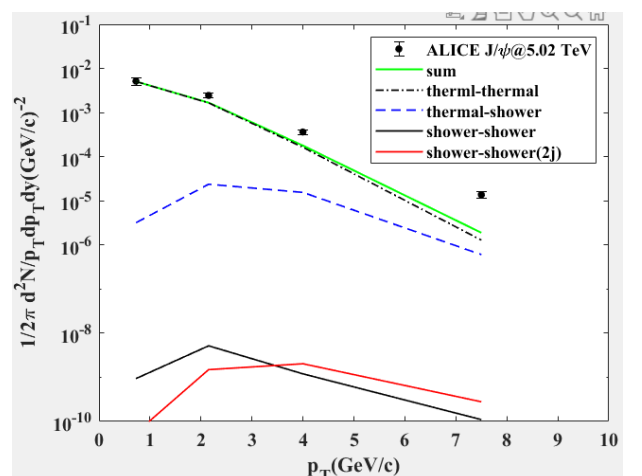
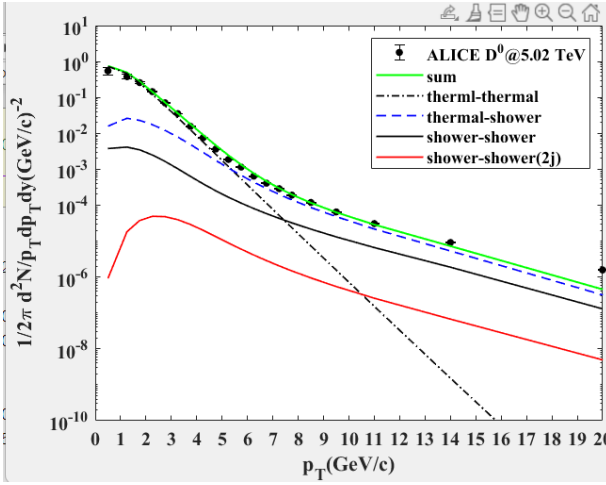
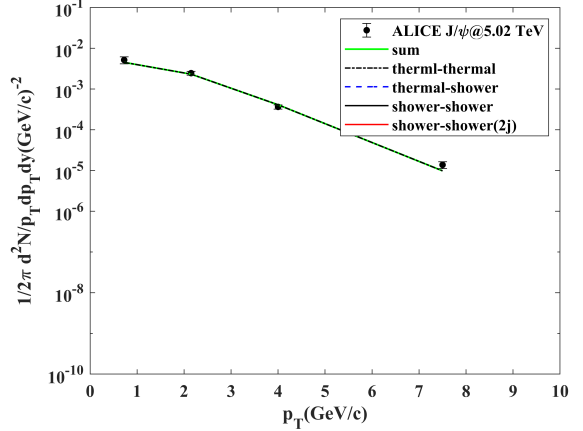
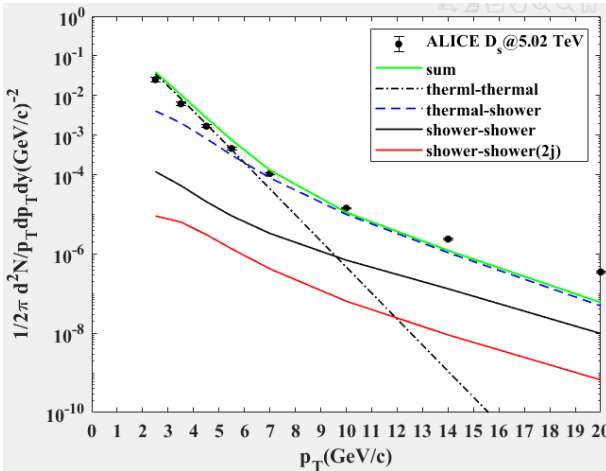
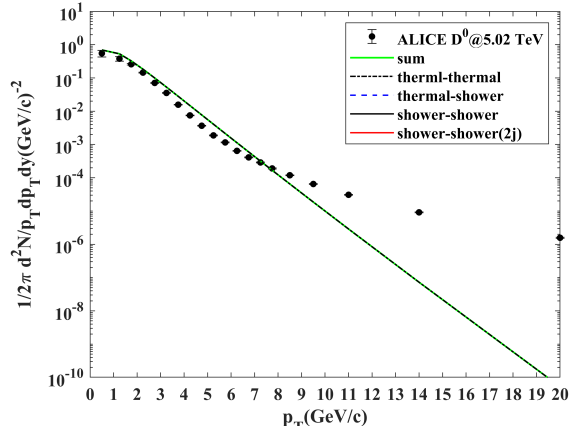


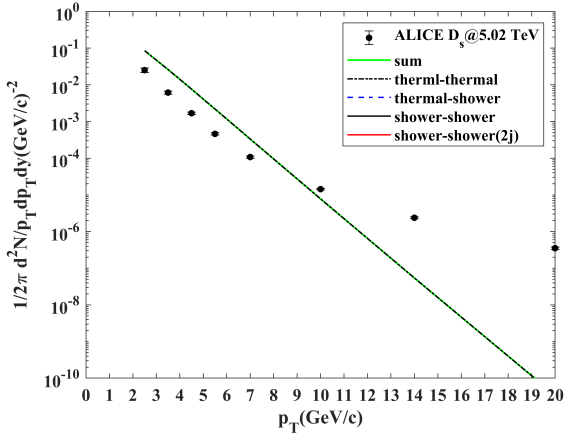
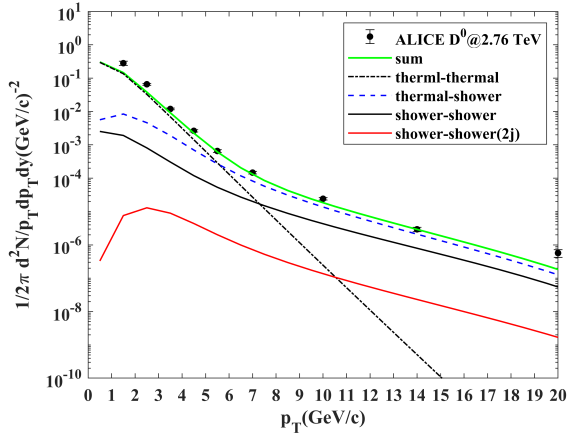
FIG. 85: J/ψ distribution at 5.02 TeV.

TABLE I: Parameters used in v16, in which γ_0 and q_0 are only for charm quark.

	C_q	T_q	C_s	T_s	C_c	T_c	γ_0	q_0	$g_{J/\psi}$	g_{D^0}	g_{D_s}
2.76 TeV	23.2	0.39	11.0	0.51	1.8	0.65	1.7	10.8	0.04	1	0.5
5.02 TeV	22.0	0.42	10.0	0.545	2.5	0.70	2.0	10.8			

FIG. 86: D^0 distribution at 5.02 TeV.FIG. 88: J/ψ distribution at 5.02 TeV with $C_c = 2.1, T_c = 0.9$.FIG. 87: D_s distribution at 5.02 TeV.FIG. 89: D^0 distribution at 5.02 TeV with $C_c = 2.1, T_c = 0.9$.

It seems the agreement for J/ψ at 5.02 TeV is not good. However, the better parameters $C_c = 2.1, T_c = 0.9$ for J/ψ are not suitable for the other two mesons, showed below.

FIG. 90: D_s distribution at 5.02 TeV with $C_c = 2.1, T_c = 0.9$.FIG. 92: D^0 distribution at 2.76 TeV.

XXIV. MEETING 2023.06.12

In our fitting strategy, T_c and C_c are first determined by fitting with spectrum of J/ψ , where TT dominates in the range of 0 to 7 GeV/c. Then g_M can be determined by fitting the components of TT for various mesons. Eventually, γ_0 and q_0 should be fine-tuned by fitting the components of TS .

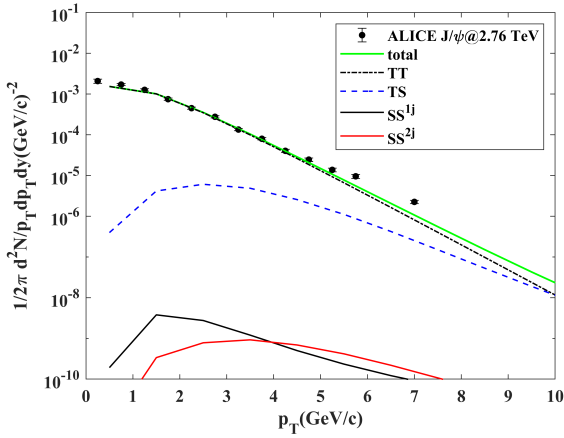
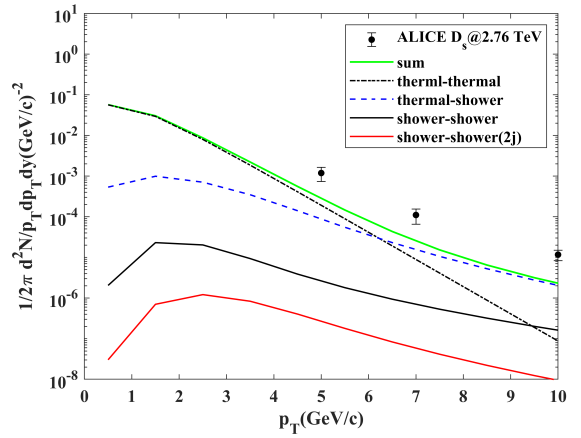
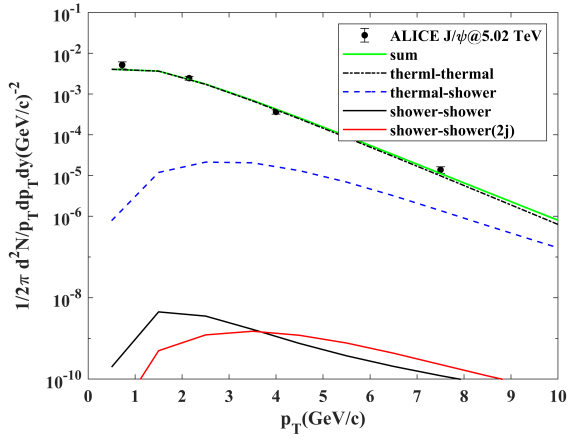
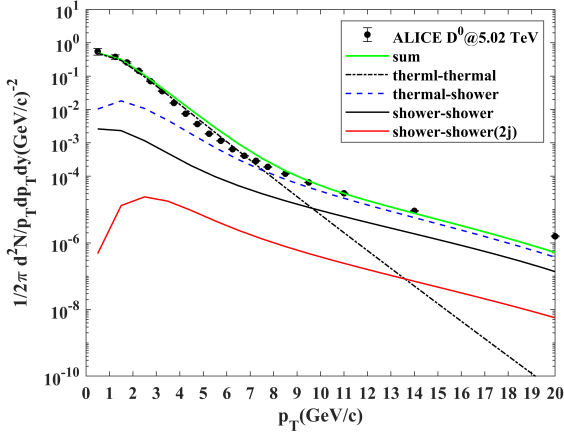
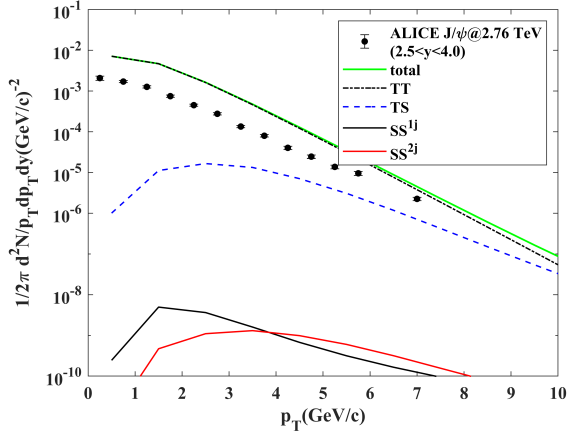
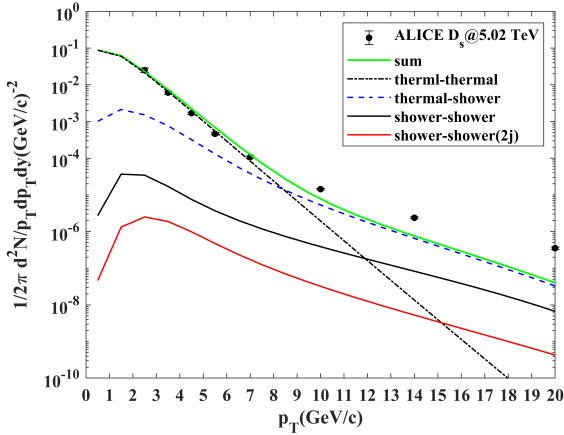
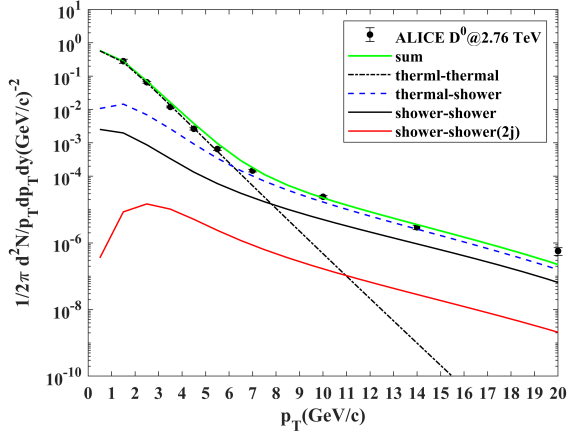
FIG. 91: J/ψ distribution at 2.76 TeV.FIG. 93: D_s distribution at 2.76 TeV.FIG. 94: J/ψ distribution at 5.02 TeV.

TABLE II: Parameters used in v16, in which γ_0 and q_0 are only for charm quark.

	C_q	T_q	C_s	T_s	C_c	T_c	γ_0	q_0	$g_{J/\psi}$	g_{D^0}	g_{D_s}
2.76 TeV	23.2	0.39	11.0	0.51	1.4	0.7	3.0	7.0	0.04	0.7	0.2
5.02 TeV	22.0	0.42	10.0	0.545	2.1	0.9	3.0	7.0			

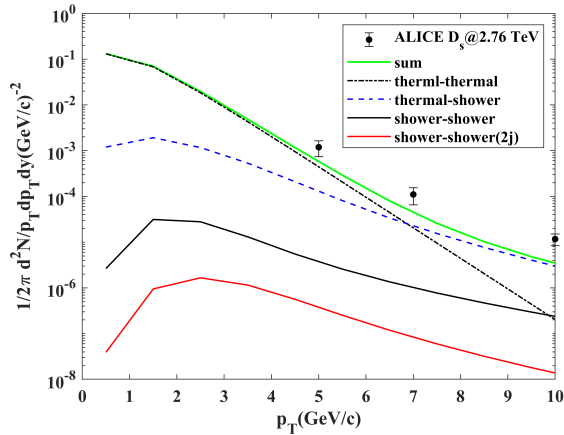
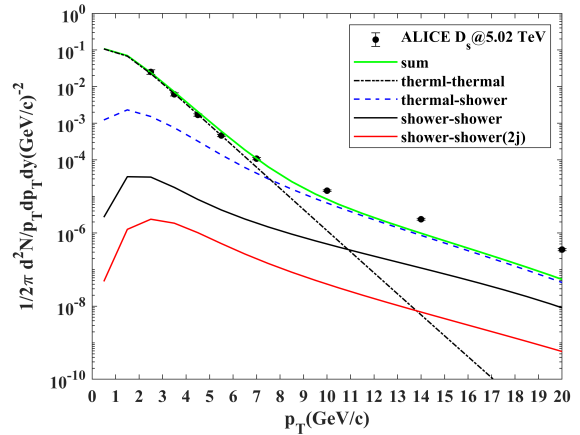
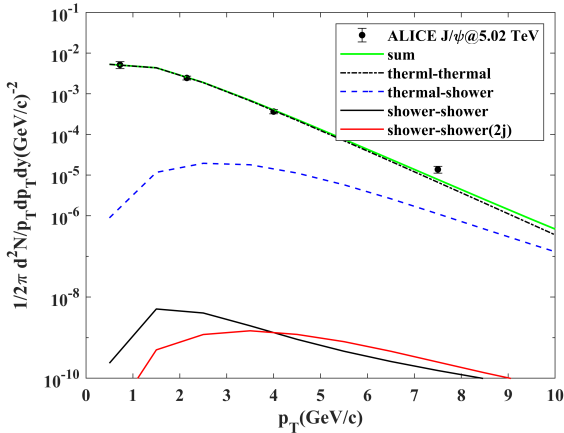
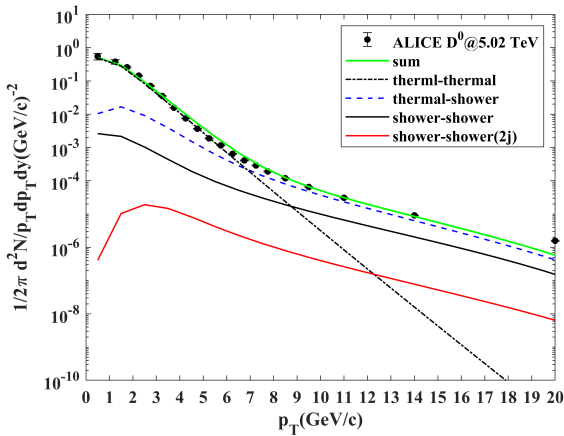
FIG. 95: D^0 distribution at 5.02 TeV.FIG. 97: J/ψ distribution at 2.76 TeV.FIG. 96: D_s distribution at 5.02 TeV.FIG. 98: D^0 distribution at 2.76 TeV.

XXV. MEETING 2023.06.19

Last week, we found the data of J/ψ at 2.76 TeV are not at mid-rapidity, which gives $2.5 < y < 4.0$. And R_{AA} , related with parameter q_0 , are given in [5–9]. After scanning, latest parameters are given below.

TABLE III: Parameters used in v16, in which γ_0 and q_0 are only for charm quark.

	C_q	T_q	C_s	T_s	C_c	T_c	γ_0	q_0	$g_{J/\psi}$	g_{D^0}	g_{D_s}
2.76 TeV	23.2	0.39	11.0	0.51	2.7	0.7	2.8	6.7	0.05	0.7	0.24
5.02 TeV	22.0	0.42	10.0	0.545	2.2	0.83	3.9	5.8			

FIG. 99: D_s distribution at 2.76 TeV.FIG. 102: D_s distribution at 5.02 TeV.FIG. 100: J/ψ distribution at 5.02 TeV.FIG. 101: D^0 distribution at 5.02 TeV.

-
- [1] D. K. Srivastava, C. Gale, and R. J. Fries, “Large mass dileptons from the passage of jets through a quark gluon plasma,” *Physical Review C*, vol. 67, no. 3, mar 2003. [Online]. Available: <https://doi.org/10.1103/2Fphysrevc.67.034903>
- [2] C. M. Ko and W. Liu, “Suppression of heavy quarks in heavy-ion collisions,” *Nuclear Physics A*, vol. 783, no. 1, pp. 233–240, 2007, proceedings of the 2nd International Conference on Hard and Electromagnetic Probes of High-Energy Nuclear Collisions. [Online]. Available: <https://www.sciencedirect.com/science/article/pii/S0375947406008232>
- [3] L. Zhu and R. C. Hwa, “A unified study of the production of all identified hadrons over wide ranges of transverse momenta at LHC,” *Journal of Physics G: Nuclear and Particle Physics*, vol. 47, no. 5, p. 055102, mar 2020. [Online]. Available: <https://doi.org/10.1088/1361-6471/ab6edf>
- [4] The ALICE collaboration., Adam, J., Adamová, D. et al. Differential studies of inclusive J/Ψ and $\Psi(2S)$ production at forward rapidity in Pb-Pb collisions at $\sqrt{s_{NN}}=2.76$ TeV. *J. High Energ. Phys.* 2016, 179 (2016). [https://doi.org/10.1007/JHEP05\(2016\)179](https://doi.org/10.1007/JHEP05(2016)179)
- [5] **ALICE** collaborations, S. Acharya et al, “Centrality and transverse momentum dependence of inclusive J/Ψ production at midrapidity in Pb-Pb collisions at $\sqrt{s_{NN}}=5.02$ TeV,” *Physics Letters B*, vol. 805, p. 135434, 2020. [Online]. Available: <https://www.sciencedirect.com/science/article/pii/S0370269320302380>
- [6] The ALICE collaboration., Adam, J., Adamová, D. et al. Transverse momentum dependence of D-meson production in Pb-Pb collisions at $\sqrt{s_{NN}}=2.76$ TeV. *J. High Energ. Phys.* 2016, 81 (2016). [https://doi.org/10.1007/JHEP03\(2016\)081](https://doi.org/10.1007/JHEP03(2016)081)
- [7] The ALICE collaboration., Acharya, S., Adamová, D. et al. Prompt D^0 , D^+ , and D^{*+} production in PbPb collisions at $\sqrt{s_{NN}} = 5.02$ TeV. *J. High Energ. Phys.* 2022, 174 (2022). [https://doi.org/10.1007/JHEP01\(2022\)174](https://doi.org/10.1007/JHEP01(2022)174)
- [8] The ALICE collaboration., Adam, J., Adamová, D. et al. Measurement of D_s^+ production and nuclear modification factor in Pb-Pb collisions at $\sqrt{s_{NN}}=2.76$ TeV. *J. High Energ. Phys.* 2016, 82 (2016). [https://doi.org/10.1007/JHEP03\(2016\)082](https://doi.org/10.1007/JHEP03(2016)082)
- [9] **ALICE** collaborations, S. Acharya et al, “Measurement of prompt D_s^+ -meson production and azimuthal anisotropy in Pb-Pb collisions at $\sqrt{s_{NN}}=5.02$ TeV,” *Physics Letters B*, vol. 827, p. 136986, 2022. [Online]. Available: <https://www.sciencedirect.com/science/article/pii/S0370269322001204>
- [10] W. Liu and R. J. Fries, *Phys. Rev. C* **78**, 037902 (2008) doi:10.1103/PhysRevC.78.037902 [arXiv:0805.1093 [nucl-th]].
- [11] R. Peng, C. B. Yang and C. B. Yang, *Phys. Scripta* **84**, 035202 (2011) doi:10.1088/0031-8949/84/03/035202 [arXiv:1103.3346 [hep-ph]].
- [12] L. Zhu and R. Hwa, “Centrality and transverse momentum dependencies of minijets and hadrons in au-au collisions,” *Physical Review C*, vol. 88, 07 2013.
- [13] R. C. Hwa and L. Zhu, “Spectra of identified hadrons in pb-pb collisions at 2.76 tev at the cern large hadron collider,” *Phys. Rev. C*, vol. 84, p. 064914, Dec 2011. [Online]. Available: <https://link.aps.org/doi/10.1103/PhysRevC.84.064914>
- [14] R. Peng and C. B. Yang, “Productions of heavy flavored mesons in relativistic heavy ion collisions in the recombination model,” *International Journal of Modern Physics E*, vol. 20, no. 5, pp. 1213–1226, May 2011. doi: 10.1142/S0218301311018356. url: <https://doi.org/10.1142/S0218301311018356>.
- [15] R. Peng and C. B. Yang, “Production of baryon-antibaryon pairs in relativistic heavy ion collisions with the recombination model,” *Nuclear Physics A*, vol. 837, no. 3-4, pp. 215–224, Nov. 2010. doi: 10.1016/j.nuclphysa.2010.05.057.